Development of an Online Monitoring and Sampling Scheme for Recombinant Protein Production

by
Louise Bengtsson

Division of Biotechnology
Lund University
September 2018

Supervisor: **Assoc. Prof. Martin Hedström**
Co-Supervisor: **Assoc. Prof. Carl Grey**
Examiner: **Dr. Javier A Linares-Pasten**

Abstract

During the past few years the focus on bioprocess monitoring and control has increased. An area still under intensive development is the sampling methods for efficient and rapid analysis during fermentations. In this thesis, an online-sampling and monitoring scheme was developed using the versatile automated continuous flow system (VersAFlo) for recombinant protein production. From the implementation of the scheme with a fermentation, recovery of intra-cellular protein occurred within 19 minutes. The binding and washing buffer were determined to be efficient at 30 mM imidazole. A second studied aspect, cell-lysis using the VersAFlo, resulted in observed trends on microliter scale (1:1 and 1:2 cells to BugBuster Master Mix ® and time intervals 0, 30, 60 120, 240 seconds). Increasing the ratio and prolonging the reaction time resulted in greater degree of lysate whilst remaining on a scale consisting of microliters and seconds. Additionally, a dilution translation tool was created for optical density measurements at 620 nm using the system set-up. A strong correlation was observed between the translation tool and external online OD measurements from the fermentations. All studies build on the creation of running schemes which are broken down into step-by-step guidelines.

Acknowledgement

The author wishes to express gratitude to all the individuals who made a difference in completing this thesis. First and foremost, to my supervisor Associate Professor Martin Hedström (Department of Biotechnology, Lund University), thank you for the guidance, immense knowledge, and inspiring ideas for this thesis. I am very grateful for the opportunity and support to work within this field, learning more techniques and developing my own scheme. Thank you to my co-supervisor, Associate Professor Carl Grey (Department of Biotechnology, Lund University) for his encouragement and help in biotechnological matters. To Zubaida Gulshan Kazi (Doctoral student, Department of Biotechnology, Lund University) and Adel Abouhmad (Doctoral student, Department of Biotechnology, Lund University), for sharing your knowledge and support for the fermentation of the organism, to Christina Wennerberg (Research Engineer, Department of Biotechnology, Lund University) for your advice and help with the ELISA, and Josefin Ahlqvist (Doctoral student, Department of Biotechnology, Lund University) for helping with various laboratory tasks, thank you all for your unwavering efforts. My sincere thanks to Dag Erlandsson (CapSenze) for the help with technical questions regarding the VersAFlo, to Frans-Peder Nilsson (Department of Biotechnology, Lund University) for the assistance in technical areas as well as biotechnological questions. To Professor Emeritus Bo Mattiasson (Department of Biotechnology, Lund University), thank you for your encouraging words and wisdom. Finally, my heartfelt thanks go to my friends and family for their support and enthusiasm through this monumental journey.

Content

1. Introduction

One of the main strengths related to utilization of online monitoring and control of a bioprocess is the high reproducibility (Kumar, Mazlomi, Hedström, & Mattiasson, 2012). Described by Kumar and co-workers, flexible monitoring systems can employ different configurations of the analytical set-up. However, sample preparation and sampling are often overlooked due to time-restraints (Luo & Pawliszyn, 2000). Concerns stated by the authors include factors such as sample loss and contamination risks.

1.1 Regulations and Directives

The EudraLex, produced by the European Commission of Health and Consumers Directorate-General, uses good manufacturing practice (GMP) which builds on the directives 2003/94/EC (human utilized medical products) and 91/412/EEC (veterinary utilized medical products) (European Comission Health and Consumers Directorate-General, 2011). GMP guidelines contains general instructions for sampling management (European Commission Health and Consumers Directorate-General, 2014). According to the European Commission, a lifted point is that each gathered sampling is to be representative of the sampling origin (European Comission Health and Consumers Directorate-General, 2011).

In 2004, the Food and Drug Administration of the U.S. Department of Health and Human services published the Process Analytical Technology (PAT) initiative. PAT is relevant for industries involving pharmaceutical development, manufacturing, and quality assurance. The document acts as a guidance to aid the development of industrial innovation and regulatory decisions involving risks. PAT can be implemented to achieve current good manufacturing practice and chemistry (cGMP) manufacturing and control (CMC). Amongst the aspirations of PAT is continuous real time quality assurance. Secondly, PAT strives for effective and efficient manufacturing process that are designed to secure performance and product quality (U.S. Food and Drug Administration, 2004). Bioprocess monitoring can incorporate a flow-injection analysis (FIA) system (Nilsson, Håkansson, & Mattiasson, 1992).

1.2 Flow Injection Analysis & Fluid Mechanics

First defined in 1978, flow injection analysis is built on three important components: sample injection, transportation/reaction, and detection (Růžička & Hansen, 1978). Listed by Růžička & Hansen, important factors of FIA are the reproducibility and controlled dispersion. Sample injection involve the process of retrieving a sample from a vessel and adding a sample plug to the system without agitating the current stream (Růžička & Hansen, 1978). A simple flow injection system, described by Růžička & Hansen (1978), could consist of a pump, a reaction coil, a flow-through detector and a waste. The stream is set in motion by the pump, a sample solution is added through a sampling port, sent through the reaction coiled and ultimately taken up into the flow-through detector.

Růžička and co-workers (1978) formulated several rules using the theory of dispersion as foundation. The first rule stated by the authors are that the dispersion decreases in small tubes if the flow rate is lowered. Treated in the fifth rule by the Růžička & Hansen (1978) is the sample zone dispersion, where the increase of dispersion of a sample zone is equal to the square root of either the residence time or the distance the sample travels. The authors note that the increase occurs when the pump rate is increased. Recommended by the sixth rule listed by the authors, the lines should be short and have an equal diameter to maintain a low dispersion by the flow, Df. On the other hand, the authors lift that the rule also mentions that a smaller sample volume allows dilution of very concentration samples (Růžička & Hansen,1978).

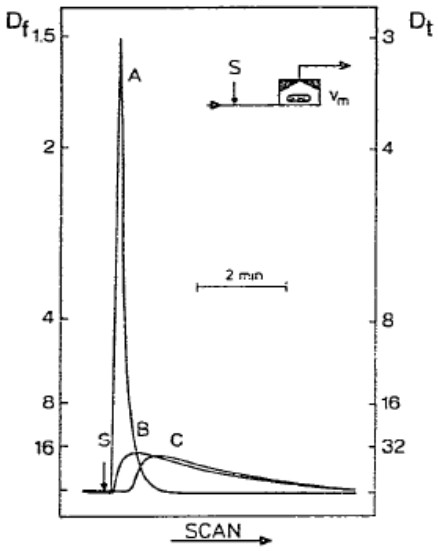

Figure 1. The effects of adding a mixing chamber to the system increases the dispersion by the flow (Růžička & Hansen, 1978)

The sample zone is affected by the Reynolds number (Re) (McKelvie, 2008). Mentioned by the authors, the Re is strictly below 2000 (<< 2000) if the internal diameter is within the interval 0.3-1.0 mm, resulting in a laminar flow. Subsequently, dispersion is mainly dictated by axial convection (McKelvie, 2008). A laminar flow implies that the mixing is limited to diffusion, thus the time requirements for sufficient mixing can be very high (Squires & Quake, 2005). The Dean number is used to express the secondary flow resulting from pipe curvature and can be described as relating the curvature ratio to the flow's Reynold's number (Patil, Nadar, & Alir, 2017). According to Růžička & Hansen (1978) the resulting response curve from the controlled dispersion changes form as the flow downstream progresses. The authors list that the shape of the sample zone can be limited to three main shapes: asymmetrical shape, symmetrical shape, and finally a Gaussian shape. The dispersion can be altered by variating the flow parameters as parameter attenuation permits optimization of the system regarding reducing time and reagent costs (Růžička & Hansen,1978).

Furthermore, depending on the factors that are to be analysed, Růžička and Hansen (1978) conclude that the composition of the sample zone is important. Limiting the dispersion of the sample plug, permits the original composition to be investigated (Růžička & Hansen,1978). However, if the purpose is to measure e.g. a change in pH or complex formation, the authors note that the sample zone must be subjected to medium dispersion. In addition, the dispersion caused by the flow is increased by adding a mixing zone prior to detection causes a voraciously increased the dispersion by the flow (D_f) (Figure 1) (Růžička & Hansen,1978).

A FIA system can be applied both for offline and online analysis, where in the online set-up both the detector and data acquisition, allowing monitoring of the broth (Kumar, et al., 2001). An example of the application of bioprocess monitoring is the monitoring of protein separation in chromatography (Nilsson, Håkansson, & Mattiasson, 1992). The authors displayed that the mode of operation can be altered to suite the type of analysis, e.g. direct assay or sequential competitive assays.

1.3 Fermentation Concepts

An alternative application where bioprocess monitoring is needed is the fermentation of bacteria, e.g. *Escherichia coli* (*E.coli*) (Ahlqvist, et al, 2016). *E.coli* grown in Luria-Bertani broth has a generation time of 20 minutes which occurs during the steady-state growth of the cells (Sezonov, Joseleau-Petit, & D'Ari, 2007). However, the growth rate is reduced by the incorporation of a foreign protein during recombinant protein production (Bentley, et al, 1990). Another factor considered by Bentley and co-workers, is that the growth rate is affected by the type of media used in combination with expression of the foreign protein. Exchanging the media from a rich media to a minimal media causes a decrease in growth rate (Bentley, et al, 1990).

The production of recombinant protein is the highest after induction using compounds such as Isopropyl β-D-1-thiogalactopyranoside (IPTG) (Mazlomi, Hedström, & Mattiasson, 2010). It has been documented by the authors that a lower amount of recombinant protein production can be observed before induction. There are two commonly used techniques of initiating the protein production of a recombinant organism (Studier, 2005). The first used by Studier (2005) is by adding an inducer, e.g. IPTG, whilst the second option, is an auto-induction approach where lactose and glycerol are added during the inoculation.

During the inoculation step of the selected strain, Studier (2005) added the auto-induction step where the glucose concentration in the reactor is lower to allow the uptake of lactose as the monosaccharide normally inhibits the lactose induction. Additionally, raised by the author, aeration is also a factor that affects the lactose uptake, where higher aeration rates can hinder the uptake of lactose if the lactose concentration is too low. Studier (2005) discussed that the production of protein, and growth of the host cell, is improved by the addition of a second carbon source. The author motivated the incorporation of glycerol as a supplement for the energy and carbon demands without hindering lactose, and thus the induction process. It has been observed that the addition of glycerol, in comparison with only using lactose, increased the quantity of produced target protein to twice the size of the latter outcome (Studier, 2005).

High-density cultivation results in a higher ratio of produced target protein per volume culture when auto-induction is implemented in comparison to using IPTG induction (Studier, 2005). Additionally, there are economic benefits to using lactose instead of IPTG as IPTG is as more expensive induction reagent (Hoffman, et al. 1995).

The process of lysing microbial cells for the release of soluble proteins comes in many forms such as mechanic, chemical and enzymatic explored by Listwan et al. (2010). Among the chemical lysis raised by the authors are BugBuster and SoluLyse, for enzymatic processes lysosome is used, whilst the mechanic process uses sonication. Evaluated by Listwan et al. (2010), the degree of soluble proteins released during the lysis depends on what method is chosen. Previous experiments performed using *E.coli* showed that sonication yields the highest amount of soluble proteins. From the results of Listwan et al. (2010), lysozyme and BugBuster displayed a lower insolubility in comparison as a result of the insolubility of larger proteins in these two methods. Lysis using SoluLyse presented competitive results with sonication (Listwan, et al., 2010).

A common technique used post cell lysis and prior to purification is clarification by centrifugation (Wingfield, 2014). If the protein contains a His-tag, then immobilized metal affinity chromatography (IMAC) can be used where the bound protein is then eluted by a buffer containing Tris, Imidazole and NaCl (Mazlomi, Hedström, & Mattiason, 2010). Non-specific

binding of proteins other than the target protein can occur, a problematic situation which can materialize if the cellular protein contains histidine (Schmitt, Hess, & Stunnenberg, 1993). Highlighted by the Schmitt et al. (1993), histidine transpires in 2% protein residues. Contamination by untagged proteins in the elute is lower in *E.coli* than e.g. mammalian systems as the occurrence of proteins with histidine residues is less frequential (Crowe, et al., 1994).

The binding of the protein is followed by a washing step and an elution step, where the washing step is completed when the absorbance (280 nm) is approximately zero, Teeparuksapun et al. (2012). According to the researchers, an absorbance of zero indicates that all components that haven't bound strongly to the Cu-IDA, such as proteins lacking the His_6-tag or a surface accessible His_6-tag, have been removed. The elution buffer contains a high concentration of imidazole, 200 mM, to elute the remaining tightly bound His_6-tagged proteins (Teeparuksapun, et al., 2012).

The strength of imidazole in the binding buffer can vary between 20 mM and 40 mM whilst the elution buffer can have a strength of 500 mM (GE Healthcare, n.d.). GE Healthcare (n.d.) recommend the HisTrap column (IMAC column) to be equilibrated with at least 5 column volumes and wash with 10-15 column volumes after sample injection. For a one-step gradient, five column volumes of elution buffer are recommended (GE Healthcare, n.d.).

A recombinant protein that can be produced by the *E.coli* BL21 strain is protein G from *Streptococcus,* where the recombinant protein G used by Zhang et al. (2015) lacks both cell surface binding sites and albumin. Through the removal of the two mentioned components the authors noticed that non-specific binding and cross reaction was lowered. In comparison with the *Streptococcal* protein G and *Staphylococcus* protein A, recombinant protein G resultingly has a higher binding capacity to immunoglobulins (Zhang, et al., 2012).

1.4 Analytical Tools

An analytical tool that has been used for protein profiling is sodium dodecyl sulphate polyacrylamide gel electrophoresis (SDS-PAGE), used for molecular weight determination where proteins are distinguished after molecular mass (Laemmli, 1970). Another variety of analysis is direct ELISA (enzyme-linked immunosorbent assay) where the plate is first coated with the antigen and the antibody (Nouri, Ahari, & Shahbazzadeh, 2018). The authors used the technique for the detection of enterotoxin A. The antibody can be an HRP (horseradish peroxidase) conjugated which changes colour from the addition of TMB substrate (Lu, et al., 2012). Lu et al. (2012) used a microplate reader at 450 nm and 650 nm measured the resulting change in colour.

Capacitive immunosensors have been employed for quantification of proteins during recombinant production from *E.coli* (Teeparuksapun, 2012). According to the authors, monitoring of the protein concentration is possible during both cultivation and downstream treatment. Capacitive biosensors are very sensitive and can have a linear range of 10^{-18} (M) to 10^{-13} (M) (Ertürk et al, 2018). Ultimately, the collected sample is to reflect the state of the cells in the reactor and improper treatment of the samples gives a false result (Picque & Corrieu, 1992).

1.5 Bioprocess Monitoring and Applications

A strength of bioprocess control systems is the reproducibility, flexible monitoring systems can employ different configurations of the analytical set-up (Kumar, et al., 2012). An example of the implementation of online bioprocess monitoring was the applied control of a bioprocess for measuring parameters such as the specific growth rate of a cell culture (Dabros, Schuler, & Marison, 2010). For sample uptake, a double lumen catheter can be used which consists of an inner and outer tube through which an inhibiting solution is pumped out of the latter tube (Mazlomi, Hedström, & Mattiasson, 2010). The inhibiting solution and the pulled-up sample are blended, where the authors noted that the determination of the feed rate is vital to prevent the inhibiting solution from being transported through the vessel. Mazlomi et al. (2010) concluded that the contamination occurs when the flow rate of the feed is too rapid. Previously it has been determined that the upper limit for avoiding contamination of the reactor with the inhibiting solution is at pump rate of 250 µl/min and a lower limit of total flow rate of 1 ml/min (Mazlomi, et al., 2010).

According to Dabros, Schuler, & Marsion (2010), different controller types can be used to control the cell culture such as feed-forward control, proportional feedback and proportional-integral feedback. A few different types of FIA set-ups for monitoring specific molecules exist, including the usage of Flow-ELISA (Nilsson, et al., 1992) and detection using enzymatic reactions and electrochemical flow-through cells (Collins, et al., 2001). From the company CapSenze Biosystems AB (Lund, Sweden), other studies have previously been made by implanting the sample monitoring products from the company (Glifberg & Svensson, Lund University, non-published work). In the case of impurity monitoring there has been an increasing need of monitoring impurities during fermentations. According to Kumar et al. (2001), time delays between sampling and results, and the lack of proactivity to hinder failed fermentation, are a part of the current situation. In addition, there can be a time delay in waiting for a pathologist to arrive and analyse why a fermentation failed (Kumar, et al., 2001).

1.6 Aim and Limitations

The aim of this project is to develop an online monitoring scheme for sampling during fermentation involving His-tagged protein G production using the innovative VersAFlo system (CapSenze Biosystems AB) to contribute to the recommendations of the FDA on advancements in the pharmaceutical industry. As previously presented in the introduction there are grounds for development of automatic sampling and monitoring techniques, of which time is one important criterium for potential real-time monitoring. Different aspects of the online sampling system are evaluated covering a binding study, lysis study and dilution study. The application of the VersAFlo in all studies contribute to the robustness determination of the system. Out of the scope of this project is the in-depth analysis of the functionality of the recombinant protein or further analysis of the bioreactions during the fermentation.

2 Experimental

2.1 Materials

The following chemicals were utilized during the studies.

- PBS Tablets (Medicago, Uppsala, Sweden)
- Glycine (Merck, Solna, Sweden)
- Zinc sulfate heptahydrate (Sigma-Aldric, Stockholm, Sweden)
- Iron(II) chloride tetrahydrate (Merck, Solna, Sweden)
- Manganese (II) sulfate monohydrate (Merck, Solna, Sweden)
- Cobalt (II) chloride hexahydrate (Sigma-Aldrich, Stockholm, Sweden)
- EDTA disodium salt dihydrate (Na2EDTA) (Merck, Solna, Sweden)
- Imidazole (Applichem, Maryland Heights, MO, USA)
- Di-potassium hydrogen phosphate (Scharlau, Barcelona, Spain)
- Tris enzyme grade (USB Amersham Lifescience, Cleveland, OH, USA)
- Super aqua blue ELISA substrate (ThermoFisher Scientific, Stockholm, Sweden)
- Di-ammonium hydrogen citrate (Merck, Solna, Sweden)
- Ammonium sulfate (Merck, Stockholm, Sweden)
- Di-potassium phosphate from Merck (Solna, Sweden)
- Sodium hydroxide from Duchefa Biochemie (Haarlem, The Netherlands)
- ClearLine DES 70 from Solveco (Rosersberg, Sweden)
- Ethanol 99.5% from Solveco (Rosersberg, Sweden)
- Ammonia 28% from VWR Chemica (Spånga, Sweden)
- Magnesium sulfate anhydrous (Sigma-Aldrich, Stockholm Sweden)
- Calcium chloride dihydrate (Merck, Solna, Sweden)
- Cupric sulfate pentahydrate from (Merck, Solna, Sweden)
- PBS – Tween Tables (Medicago, Uppsala, Sweden)
- Sodium Dodecyl Sulfate (SDS) (Promega, Nacka, Sweden)
- Running Buffer (10 ml 10 % SDS, Glycine, Tris) (DI)
- Sample Buffer: Tris, SDS, glycerol, bromophenol blur 0.2% w/v, dithiotreithol Milli-Q-water
- Staining Buffer
    - Coomassie
    - Methanol
    - Acetic Acid
    - Milli-Q-water
- Destaining Buffer
    - Acetic acid 10%
    - Methanol 40%
- Protein G (Indienz AB, Billeberga, Sweden)
- Protein G (GenScript, Stockholm, Sweden)
- Molecular Weight Ladder (Bio-Rad, Solna, Sweden)
- MQ-water (Millipore)
- DI-water
- D(+)-Glucose 1-hydrate (Biochemica, Billingham, United Kingdome)

- Lactose (Fluka, Bucharest, Romania)
- Precision Plus Proteins, all blue standards (Bio-Rad, Solna, Sweden)
- Ampicillin sodium (Duchefa Biohcemie, Haarlem, The Netherlands)
- Polyclonal swine – anti rabbit/ HRP (Agilent, Kista, Sweden)
- Bovine-Serum, Albumin 99% (Sigma-Aldrich, Stockholm, Sweden)
- Glycerol (Sigma-Aldrich, Stockholm, Sweden)
- Ampicillin resistant *E.coli* producing recombinant protein G
- BugBuster® Master Mix (Novagen, Merck, Solna, Sweden)
- IMAC beads (Ni-NTA)(Bio-Works AB, Uppsala, Sweden
- 37% Hydrochloric acid fuming (Merck, Solna, Sweden)

2.2 Hardware

The versatile automated continuous flow system, VersAFlo, developed by Capsenze Biosystems AB contains two Cavro Centris pumps from Tecan (Männedorf, Switzerland). Each pump is connected to a Tecan 12-port Cavro smart valve via an injection loop connected to one of the pump's three ports. The VersAFlo also contains a bioreaction cassette system, a degasser unit from Biotech (Onsala, Sweden) and two flow-based spectrophotometric detectors; an internal UV-detector from Runge (Bremen, Germany) and a VUV40 from Visacon (Salt Lake City, UT, USA) respectively. In addition, the VersAFlo instrument contains three 3-way diverter valves from Asco (Florham Park, NJ, USA). Figure 2 displays the general set-up of the VersAFlo.

The two 12-port Cavro smart valve plus are connected via a tee-based confluent point. Via a dilution region, the confluent point is connected to bioreaction cassette packed with IMAC WorkBeads 40 IDA. From the column in the cassette (16 µl per column, excluding the approximately 2 µl void), the system is connected to a degasser and the UV-detector (280 nm). Two of the 3-way valves are connected, the first to the purified protein sampling tube and the second to the waste.

Additionally, from the first 12-port Cavro smart valve plus, the system is connected to a WPA Biowave 2 spectrophotometer (Biochrom, Cambridge, United Kingdom). Detection is performed via an 80 µl flow cuvette (Hellma Analytics, Müllheim, Germany). Prior to the spectrophotometer there is a dilution region. The tubes connecting the equipment are either of a 0.8 mm inner diameter or 0.25 mm diameter.

The pump for preparing the affinity column was a Minipuls 3 from Gilson (Limburg-Offheim, Germany). External pH measurements were performed with the inoLab pH Level 1 (WTW, Weilheim, Germany). The temperature of the fermentation was monitored using an EKT Hei-lon (Heidolph, Schwabach, Germany) and internal pH measured by MR Hei-Standard (Heidolph, Schwabach, Germany). The pH inside the fermenter was measured using a gel pH electrode (Mettler Toledo, Stockholm, Sweden), connected to a pH regulator (Inventron Inc, Livonia, MI, United States).

For the ELISA an ELx808 Absorbance Reader (Biotek, Winooski, VT, United States) is used. Whilst the SDS-PAGE set-up (Bio-Rad, Solna, Sweden) is connected to a voltometer. The Mini-Protein TGX Gels, 10 precast, 4-20% 10-well 30 µl, SDS-gels were used from (Bio-Rad, Solna, Sweden) and the Mini-Protein TGX Gels, 10 precast, 4-20%, 12-comb, 20 µl from (Bio-Rad, Solna, Sweden).

The weighing scales used include a New Classic MF ML104 101 (METTLER TOLEDO, Stockholm, Sweden), PB602 (METTLER TOLEDO, Stockholm, Sweden), Adventure Pro AU213C (OHAUS, Switzerland). For the glucose measurements the Accu-Chek Aviva (Roche, Solna, Sweden) with test strips were used.

2.3 Software

The dedicated VersAFlo software, developed by CapSenze Biosystems AB, controls all the VersAFlo actuators, of which the two Cavro Centris pumps (ID 1 and 3) and 12-port Cavro smart valve plus (ID 2 and 4) are categorized as Tecan-units. Several modes and positions are

possible with the Tecan-units. Tecan:0 allows for real-time monitoring of the activity of each Tecan-unit. Another type of actuators are the GPIOs. Within this category are the three 3-ways valves (ID as valve1, valve 2, and valve3), and the degasser. The GPIOs can either be activated and deactivated.

Additional actuators are the internal UV-detector and a biosensor (not implemented in this work). The internal UV-detector also includes a real-time monitoring option and can be calibrated during the run where the fluid passing the system becomes the blank.

2.4 Methods

2.4.1 Fermentation

In a high-density fermentation, recombinant protein G produced by *E.coli* can reach 1 g of protein G per 1 L of broth. This requires IPTG, Luria-Bertani medium and 2xYT medium (Zhang, et al., 2015)**.** Production of recombinant *E.coli* starts with the cultivation on an ampicillin rich agar plate and the ampicillin concentration is set to 100 mg/L and growth occurs at 37 ^{o}C (Mazlomi, Hedström, & Mattiasson, 2010).

For the fermentation the recombinant *E.coli* BL21(DE3) containing plasmid pUC19 producing His-tagged protein G was used. The interactions with immunoglobulins (Zhang, et al., 2015) and the use of a His-tag for IMAC purification (Mazlomi, Hedström, & Mattiason, 2010), where the combined main reasons for using protein G as the model recombinant protein.

The defined minimal media created by Holme et al. (1970) has been used in high cell density cultivations. The trace elements solution contains 0.5 g/L $CaCl_2$• 2 H_2O, 16.7 g/L $FeCl_3$•$6H_2O$, 0.18 g/L $ZnSO_4$•$7H_2O$, 0.16 g/L $CuSO_4$•5 H_2O, 0.15 g/L MnSO4•H_2O, 0.18 g/L $CoCl_2$•$6H_2O$, and 20.1 g/L Na_2EDTA (Holme, 1970). For the fermentation the trace elements were prepared to the concentrations above with the exception for the iron(III) chloride hexahydrate, which was recalculated and replaced by iron(II) chloride tetrahydrate. All of the trace elements were dissolved in 0.2 M hydrochloric acid.

The recipe for the salt-medium (NYAT) contains 2.0 g/L $(NH_4)_2SO_4$, 14.6 g/L K_2HPO_4, 3.2 g/L NaH_2PO_4·H_2O, and 0.5 g/L $(NH_4)_2$·H·citrate (Holst, et al, n.d.).

A stock solution of the 5X NYAT medium (5 times concentrated mineral salt medium) was prepared in DI-water. In addition to the trace elements, and 5X NYAT medium, a stock of 1 M magnesium sulfate, 50% glucose stock, 600 g/L glycerol stock, and an 8 g/100 mL lactose stock solution were autoclaved in separate containers. An ampicillin stock solution of 30 mg/mL to 100 mg/mL was prepared using Milli-Q water and added through sterile filtering.

The organism was first incubated on an ampicillin plate at 37 ^{o}C and later grown in 100 mL inoculum and stored as a glycerol stock. The inoculum was prepared in a shake flask with a final x1 dilution of the NYAT solution. Glucose, magnesium sulfate, sterilized water and trace elements were added separately. The ampicillin was added by sterile filtration to a final concentration of 100 mg/L. Autoclaved DI- water is added to the inoculum to a final total volume of 100 mL. A 1 ml *E.coli* glycerol stock is added to the shake flask. To maintain the sterility barrier, the addition of components is performed in a sterile bench. The seed medium is incubated at 37^{o}C at 200 rpm for 17 hours and 22 minutes and at 27^{o}C for 2 hours and 27 minutes.

The fermentation was performed in a 2 L bioreactor. Differing from the inoculum, the 5X NYAT medium and DI-water was added to the reactor prior to autoclavation. The NYAT medium would have a x1 concentration after adding all fermentation components if the inoculum has a volume of 60 mL. Prior to transferring the 100 ml inoculum to the reactor, glucose, magnesium sulfate, trace elements, ampicillin, lactose, glycerol are transferred to the reactor using a transferring vessel. The inoculum is transferred to the fermenter using a separate transferring vessel.

To further control the auto-induction, a set concentration of glucose of 0.05% can be added (Studier, 2005). According to Studier (2005), the glucose hinders the auto-induction allowing growth without interference of otherwise produced toxic proteins.

At the start of the fermentation, the concentrations glucose, lactose, glycerol and ampicillin are calculated to be 0.24 w/v%, 0.19 w/v%, 0.49 w/v% and 97.4 mg/L. The calculations assume that the remaining glucose and ampicillin concentrations in the inoculum are negligible.

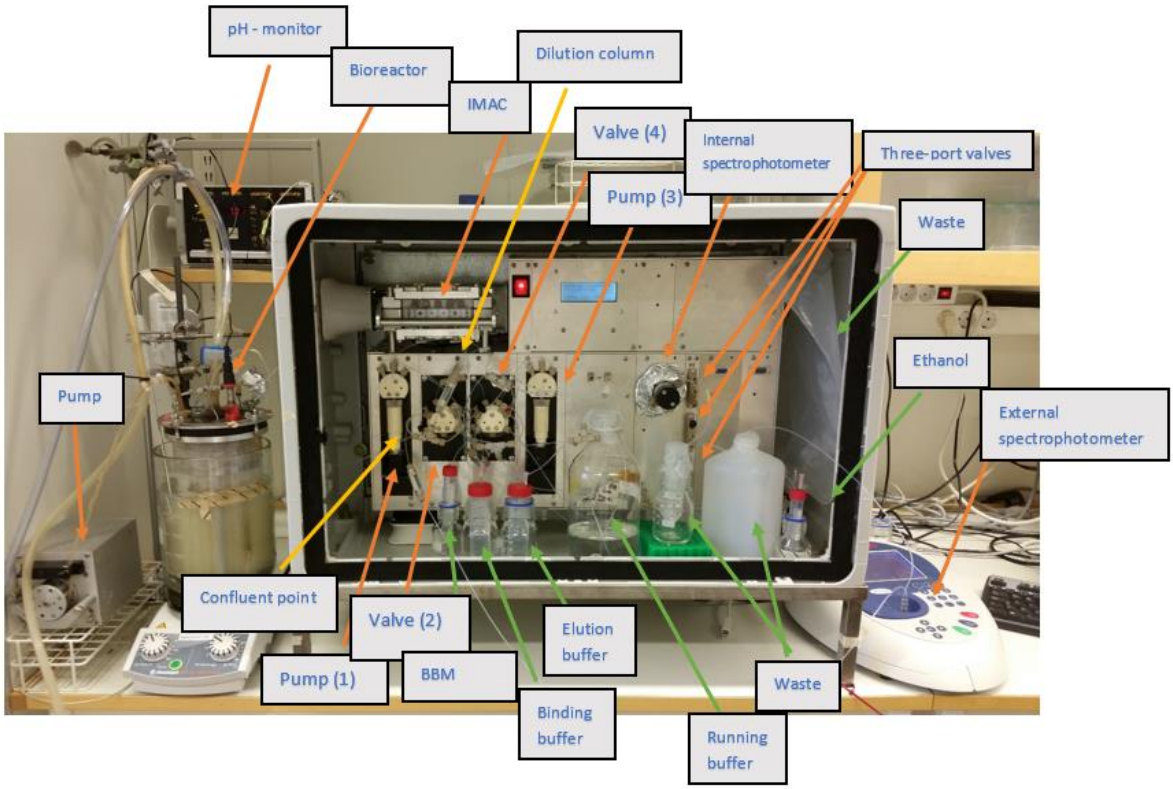

Figure 2. Experimental set-up for fermentation. Tecan ID numbers for the pumps and valves are given.

The fermentation is performed at 37 - 38 ^{o}C with a stirring speed of approximately 225 rpm (with slight variations) which was manually changed. To maintain the sterility barrier the ingoing oxygen passes a sterile filter. The outgoing carbon dioxide tubing is placed in a container with 70% ethanol.

The pH was monitored using a pH-electrode that was calibrated and fixed in the reactor prior to autoclavation. After proceeding with the fermentation, an external pH-electrode was used to update the internal pH-electrode. The internal pH-electrode was connected to regulate the feed of ammonia to the culture.

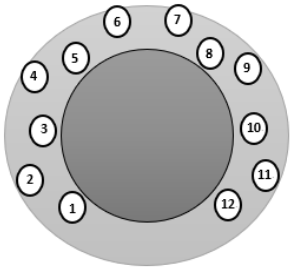

Figure 3. An illustration of the 12-port valves (Tecan 2 and 4).

During the fermentation, the pO_2 is correlated to the cell growth. As the culture increases, the oxygen requirements increase. At 10% saturation, the dissolved oxygen level is sufficient for the cells (Risenberg, et al., 1991). For this fermentation the pO_2 was not monitored thereof the manual variation of the rpm.

During the fermentation, sampling was performed every hour manually (offline) and by the VersAFlo (online). The recorded parameters from the offline sampling are: temperature, internal pH, external pH, glucose concentration, and the optical density at 620 nm. The offline sampling is performed hourly commencing with the discarding of 2ml sample. During the culture harvesting, 1.5 ml samples are taken in triplets or five 1 ml samples. The first sample is saved for further analysis, sample 2 is used for SDS-PAGE and the third sample to determine the OD and glucose concentration.

For the fermentation, the set-up can be viewed in Figure 2. An illustration of the 12-port valve is displayed in Figure 3 and the corresponding connections in Table 1.

Table 1. Decodes the connection of buffers and samples to the two 12-port valves (Tecan 2 and Tecan 4). The table includes sample (S), block (B), confluent point (CF), degasser (D), binding buffer (BB), elution buffer (EB), EtOH, OD, and BBM. If a port is not used, the port is blocked (X)**.**

Port	**1**	**2**	**3**	**4**	**5**	**6**	**7**	**8**	**9**	**10**	**11**	**12**
Valve (Tecan 2)	S	B	CF	OD	X	X	X	X	BB	X	X	EtOH
Valve (Tecan 4)	BBM	B	CF	BB	X	X	D	X	X	EB	X	EtOH

The method for online sampling builds on the resulting scheme built using the VersAFlo software. A description of the final scheme is given in the Appendix C. In summary, the loops and tubing leading through the spectrophotometer are rinsed with ethanol to reduce the risk of cross-contamination. Then sample and solutions tubes are first cleaned with ethanol the IMAC column is first equilibrated with binding buffer (30 mM imidazole in phosphate buffer saline, pH 7.4, sterile filtered) and the internal UV-detector was zero calibrated using the same buffer. A 550 µl volume of sample is first pulled in and discarded to the waste, priming the sampling tube. Another sample plug of 80, 40, 20, or 10 µl (see section: Verification of the VersAFlo Setup) is pulled in at a rate of 20 µl/s and sent to the external spectrophotometer via a dilution column, followed by running buffer (10 mM sterile filtered potassium phosphate buffer, pH 7.28).

The optical density is measured at 620 nm with an interval of 2 seconds. Succeeding the OD measurement, another 75 µl of sample is pulled in to the first valve (Tecan ID 2) with a rate of 20 µl/s to the loop that has been prepared with binding buffer. The second pump (Tecan ID 3) pulls in 150 µl of BugBuster® Mastermix (BBM) to the loop of the second valve (Tecan ID 4) already containing binding buffer. Initially, 30% of the total BBM volume is dispensed to the confluent point. Post priming the confluent point, the sample and remaining BBM are dispensed simultaneously to the confluent point to the dilution column at a rate of 5 µl/s. The other alternative running schemes use this method for lysis, however due to an irregularity in the new scheme, the second loop first pulls in 45 µl of binding buffer from the system and then dispenses 135 µl of binding buffer and BBM to the dilution chamber. Thus, the 75 µl of *E.coli*

reacts with 78 µl of BBM. An alternative sampling and elution schedule is displayed in Appendix F and estimated amount of protein G in Appendix 1.

The cell lysis is performed for 120 seconds before sending the cell broth through the IMAC column using only the second pump (Tecan 3) and valve (Tecan 4). No centrifugation, prior to protein binding, was performed to separate the soluble phase from the insoluble. Washing buffer is sent through the system at a flow of 10 µl/s. Two elution plugs (at injection 500 mM imidazole in potassium phosphate buffer, pH 7.4, sterile filtered) separated by the uptake and dispense of binding buffer. For the first two measurements, only one elution pulse of double the volume was dispensed, which was later corrected during the fermentation. The binding, washing and elution are all monitored by using the internal UV-detector and the elution peaks are sampled for 25 seconds. Prior to the next sampling hour, the path from both loops to the elute sampling tube and through the external spectrophotometer (Biowave) are cleaned with 70% ethanol. After a complete run is performed a new scheme is manually started once the reactor has been disconnected from the VersAFlo. In the new scheme all inlet sample and solution tubes are rinsed with an ethanol plug.

2.4.2 Cell Lysis

The offline samples were lysed using BBM. The cells were lysed, and the supernatant prepared for the SDS-PAGE according to the manual recommendations (Merck, n.d.). The samples were centrifuged for 10 minutes at 16.000 rcf and the liquid was removed, salvaging the cell pellet. 200 µl BBM was added to each Eppendorf tube and the cell pellets were resuspended. The cell suspension was incubated on a rotating platform for 20 minutes, after which the cells were centrifuged for approximately 16 minutes at 4 ^{o}C, until the correct temperature was reached, the centrifugal force was set to 7.500 rcf. The supernatant was thereafter transferred to separate Eppendorf tubes and stored in the freezer. Prior to freezing, 15 µl of sample and 15 µl of 4x sample buffer were mixed and heated to 85 ^{o}C for 3 minutes. The prepared supernatants were stored in the freezer until running the SDS-PAGE.

2.4.3 SDS

SDS-page used (BIO RAD, n.d. -a) a running buffer consisting of (3.03 g Tris, 14.4g glycine, distilled water) of which 10 ml of 10% SDS solution was added to. The SDS-Page protocol, Holst, et al. (n.d.), structure and changes used are as follows below. The samples were mixed with sample buffer (1:1 ratio) or (4:1 ratio) depending on the concentration of the sample buffer. After heating the samples to 100 ^{o}C for 10 minutes, the samples were centrifuged and (if needed) vortexed. Notably the protein marker was loaded directly on the SDS-gel. The samples were loaded onto the gels and run at 150 V until the bands had travelled to the bottom. Finally, the gels were placed in staining buffer for 30 minutes and then de-stained using either de-staining buffer, DI-water or fluctuating between the two.

2.4.4 ELISA

The online samples were diluted in coating buffer (1.5 g Na_2CO_3 and 2.93g $NaHCO_3$ in distilled water) (BIO RAD, n.d -b) into two types of dilutions. The first, a x2 dilution, consisted of 75 µl was diluted with 75 µl coating buffer. The second dilution was a x3 dilution. In order to maximize the amount of protein used, the first well would always contain 75 µl of the x2 dilution and the second well the remaining volume (ultimately serving as an iterative result and not quantitative found in Appendix I). Of the x3 dilution, a minimum of two well for each sample was filled. Additionally, standard solutions with estimated concentrations of 0.625 µg/ml, 1.25 µg/ml, 2.5 µg/ml, 5 µg/ml and 10 µg/ml of purified protein G stock were used.
The 96-well plate was incubated for 3 hours and 16 minutes in room temperature.

After washing several rounds with the washing buffer (10 mM phosphate buffer, 0.003 M KCl, 0.14 M NaCl, 0.05% Tween® 20) the plate was incubated in the fridge with blocking buffer (1.0% bovine serum albumin in 10 mM phosphate buffer, 0.140 NaCl, 0.0027 M KCl) (BIO RAD, n.d. -b). The plate was removed from the fridge at mid-day the following day (CUSABIO, n.d.). The plate was washed with washing buffer and incubated for a minimum of 2 hours with the polyclonal swine- anti rabbit HRP conjugate diluted in the washing buffer (CUSABIO, n.d.). During the 2 hours the 96-well plate was kept at 27 ^{o}C, and a rotational speed of 26 rpm. Super aqua blue ELISA substrate was added, and the signal measured for 2 hours in total. All buffers were filtered before usage.

2.4.5 Programming a Running-Schedule

The CapSenze software provides the user a variety of configurations and flow-scheme alternatives using the actuators above as building blocks. Furthermore, extra commands include: dwell, loop and wait.

The dwell function pauses the system for the set amount of time or until a digital time. Loop is a function where a set of blocks (sub-schemes) are repeated a set number of times, each time looping to a specified block. Wait can be used if an actuator is working in the background, e.g. two pumps performing tasks simultaneously. The system then holds the flow-scheme until the background block has completed the task.

An overview of the program options for the Tecan units relevant for this study are listed in Table 2. In Appendix A, a detailed list is given including the functions of internal UV-detector and GPIOs.

Table 2. Displays the optional parameters of the Tecans 1, 2, 3 and 4.

Parameter	Options for the Parameter	Description
Pump ID	1 or 3	Command which pump to perform the activity
Valve ID	2 or 4	Command which valve to perform activity
Direction of Movement	O or I	The active valve moves in set direction: - Anti-clockwise (O) - Clockwise (I)
Port ID	1-12	End port of designated valve
Position of Pump	O, E, I	Position of the active pump depending on desired connection: - To the loop (O) - To the Running Buffer/Water source (E) - To the Waste (I)
Mode of Pump	A, P, D	Command the pump a mode of action - Absolut (A): Sets pump to the designated volume - Pull (P): Pulls in volume equal to set value - Dispense (D): Pushes out volume equal to set value
Volume	Set a volume [µl]	Volume that the active pump is to pull in, dispense, or set as an absolute volume.
Flow	Set a flow rate [µl/s]	Define at which flow rate the volume is transported

To program the system, four main sub-schemes were used for efficient structuring of a running scheme (Appendix A, B and C). The four sub-schemes inspired by the available sub-schemes in the CapSenze software are described in brief below:

1. FillPump_ChangePort_EmptyLoop (FCE)

Commands a pump to pull in buffer and send the contents to the designated port.

2. Valve_And_Pump_Sequence (VPSe)

The active valve moves direction to desired port and either takes up or sends out the content using the set pump.

3. TakeFromPort_SendToPort_Sequence (TSSe)

The active valve changes to the inlet port, takes up the solution using the designated pump, switches port, and sends out the solution.

4. TakeUpToPump_TakeFromPort_SendToPort_Sequence (TTSSe)

Similar to TSSe, however, the active pump first takes up running buffer or water directly to the pump.

2.4.6 Fluid Mechanics

To calculate the Reynolds number (Re), Equation 1 was used) where u is the linear velocity in relation to the continuous phase, and d the length characteristics (Villadsen, Nielsen, & Lidén, 2011, pp 479). η is the dynamic viscosity (kg/(m·s)) and $\rho_1$is the liquid density (kg/m^3) (Villadsen, Nielsen, & Lidén, 2011, pp xvii)

$$Re = \left[\frac{ud\rho_1}{\eta}\right] \quad \textbf{Eq. 1.}$$

The Dean number for the curvature of the two loops was calculated by using Equation 2 which is take from displayed in Patil, Nadar, & Alir (2017).

$$D_e = R_e\sqrt{(\frac{D_i}{D})_{const.}} \quad \textbf{Eq. 2.}$$

The total dispersion is described by Equation 3 where C_0^0 is the initial concentration of the sample prior to injection, and C^{max} the concentration analogous to the maximal peak. The ratio of the two concentrations are correlated to the peak heights (H_0^0 and H) and const. stands for a conversion factor relating the signal to the concentration (Růžička & Hansen, 1978).

$$D_t = {C_0^0}/{C^{max}} = {const.\,H_0^0}/{const.\,H} \quad \textbf{Eq. 3.}$$

Equation 4 describes the dispersion where the effect of the flow rate of the carrier (Q_c) and the reagent (Q_R) (McKelvie, 2008).

$$\frac{(Q_c+Q_R)}{Q_C} = 2 \quad \textbf{Eq. 4.}$$

The system utilizes tubes to transport masses from point A to point B. Two different diameters were used (0.8 mm and 0.25 mm) with the combination of seven different volumetric flows. The dynamic viscosity and density are approximated to be equal to that of water at 20 °C, Table 3.

Table 3. The dynamic viscosity and density for water at 20 degrees (Mörtstedt & Hellsten, 1987).

Dynamic viscosity (Pa·s)	**Density (kg/m^3)**
0.001	998.2

2.4.7 Verification of the VersAFlo Setup

The verification of the VersAFlo setup is divided into four section: A binding study, lysis study, dilution determination, and fermentation implementation.

2.4.7.1 Binding Study

The binding study tested two different concentrations of binding and washing buffer (20 mM or 30 mM imidazole in 10 mM PBS), the sampling efficiency and monitoring of binding and elution.

Prior to protein injection, the IMAC column (bioreaction cassette) was equilibrated with binding buffer (800 µl) of a set concentration and the online internal UV-detector calibrated. Protein G obtained from Indienz AB (Billeberga, Sweden) was diluted to 1 mg/ml was injected into the VersAFlo at a volume of 300 µl and pushed through the column at a flow rate of 3 µl/s. 1000 µl of binding buffer followed the sample plug at 3 µl/s. In the binding study, no dilution column was used prior to binding. The bound protein was washed with washing buffer of the same imidazole concentration as the binding buffer. Two injections (minimum) of the elution buffer (100 µl/injection, 200 mM imidazole in PBS) were intermediated by a large pulse of binding buffer (800 µl) at 10 µl/s. The binding, washing and elution was followed by using the Internal UV-detector. The first elution peak was sampled for approximately 25 seconds and run on a SDS-gel along with pure protein G stock. Each imidazole concentration was repeated three times. Afterwards the path from Tecan 2 through the internal online UV-detector was cleaned with 70% ethanol.

2.4.7.2 Online Cell Lysis

A full factorial of experiments was performed for the determination and verification of the online chemical cell lysis. Two parameters were adjusted, the ratio *E.coli* cell suspension versus BBM and the reaction time of the chemical lysis.

The ratio of *E.coli* cell suspension to BBM was tested at a 1:1 ratio and 1:2 ratio with a total volume of 225 µl. A dilution column was used as a mixer connected to the external spectrophotometer measuring at 620 nm with a 2 seconds interval. The tubes from the valve to the external spectrophotometer hade a diameter of 0.8 mm and the flow from the loop to the spectrophotometer was 50 µl/s.

Prior to the sample plug being injected, a plug of BBM was first pulled in equivalent to 70 % of the total BBM volume. The remaining 30% was pulled in after the sample plug was in place. Two types of blanks were performed. The first was a blank consisting of running buffer plug and BBM, the second used a sample plug surround by running buffer.

Two parameters were investigated: the reaction time and the ratio of sample to BBM. Table 4 lists the ratios and times investigated. The results are iterative due to each combination only being performed once.

Table 4. The ratios of sample (S) to BBM evaluated. Additionally, the volumes of each plug and the reaction times are listed.

Ratio [S: BBM]	**S [µl]**	**BBM (total) [µl]**	**BBM After S (70%) [µl]**	**BBM Before S (30%) [µl]**	**Total Volume [µl]**	**Reaction Times (s)**
1:1	112.5	112.5	33.75	75.75	225	0; 30; 60; 120; 240
1:2	75	150	45	121.5	225	0; 30; 60; 120; 240

2.4.7.3 Determination of Online Dilution

The dilution column implemented in the previous study is used for the cellular OD measurements in the fermentation set-up using the online external UV-detector. To accommodate the variating samples volumes used for the OD measurements, the dilution of each used volume was studied.

Initially a stock solution of *E.coli* was diluted (x20) of which the OD at 620 nm determined to be 8.02. The sample was diluted according to Table 5 depending on the volume studied prior to injection. In addition, the initial OD of each injection is calculated based on the dilution of the original stock.

Table 5. The volumes used during the dilution determination and the dilution of the stock prior to injection are displayed. The equivalent OD depending on the dilution of the stock are calculated.

Volume [µl]	**Dilution of stock**	**Calculated OD**
10	None	8.02
20	X2	4.01
40	X3	2.67
80	X4	2.01

Measurements using the Biowave II spectrophotometer were performed every 2 seconds. The pump (Tecan 1) first pulls in running buffer. Succeeding the pump preparation, a sample plug of volume from Table 5 is pulled in to the valve (Tecan 2) at a rate of 10 µl/s. The total volume of sample and running buffer was 2800 µl. After pulling the sample into the loop, the entire loop was sent to the external spectrophotometer, via the dilution region, at a rate of 50 µl/s. A minimum of 5 repetitions of each volume was performed. Cases were bubbles are suspected to have interfered with the signal were excluded. The remaining results were checked for outliers using Equation 5 and 6.

The determination of the interquartile range (IQR) was thus calculated to determine near outliers (Spencer, Cowans, & Nicolaides, 2008). As used by Spencer et al. (2008) a data point was considered an outlier if it was larger or lower than 1.5×IQR from the lower (Q_1) and upper (Q_3) quartiles equations 5 and 6.

$$Q_1 - 1.5 \times IQR \quad \textbf{Eq. 5.}$$

$$Q_3 + 1.5 \times IQR \quad \textbf{Eq. 6.}$$

3 Results

3.1 Calculated Fluid Mechanics

The Reynolds number was calculated for each combination of the tube inner diameter and flow used in the flow injection analysis system using equation 1. Table 6 displays the calculated Reynolds numbers.

Table 6. The Diameter of the tubes, area, volumetric velocity of the flow, the calculated velocity and Reynolds numbers are displayed below.

Diameter (m)	**Area (m^2)**	**Volumetric velocity (m^3/s)**	**Velocity (m/s)**	**Re**
8.0E-4	5.03E-7	1E-7	0.199	158
8.0E-4	5.03E-7	5E-8	0.00995	79.0
8.0E-4	5.03E-7	2E-8	0.0398	31.6
8.0E-4	5.03E-7	1E-8	0.0199	15.8
2.5E-4	4.91E-8	1E-8	0.204	50.6
2.5E-4	4.91E-8	5E-9	0.102	25.3
2.5E-4	4.91E-8	3E-9	0.0611	15.2
2.5E-4	4.91E-8	1.67E-9	0.0340	8.45

The Dean number for each tube and flow combination was calculated using equation 3. Table 8 summarizes the equivalent dean numbers for the loops, the measurements for the loops are listed in Table 7.

Table 7. The measured diameter of one 12-port valve (assumed equal for both Tecan 2 and Tecan 4) and the inner diameter of the tubing looped around the valve.

Diameter Loop, D (m)	22.5×10^{-3}
Inner diameter, Di (m)	0.8×10^{-3}

Table 8. Displays the calculated Dean number for each previously calculated Reynolds number.

Re	158	79.0	31.6	15.8	50.6	25.3	15.2	8.45
De	21.1	10.5	4.22	2.11	3.77	1.86	1.13	0.629

3.2 Binding Study

An example out-take from the binding and elution of pure protein G using the 30 mM binding buffer is displayed in Figure 4. The larger peak is from the binding and washing of the column whilst the sequential peaks are from the elution buffer used to indicate when to start sampling the elute.

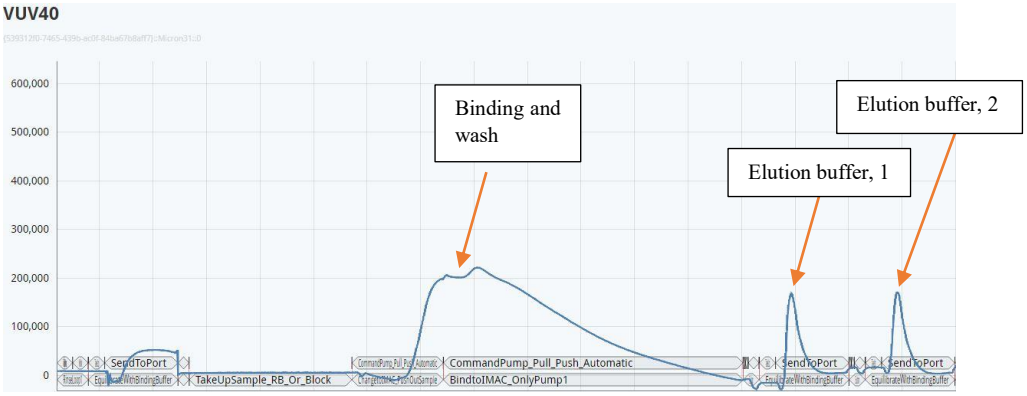

Figure 4. Binding and elution of 300 µl injected 1 mg/ml protein G. VUV40 is used as spectrophotometer instead of Micron 31.

From the binding study, the collected samples from the 20 mM binding buffer (20) experiment and 30 mM binding buffer (30) experiment yielded bands on the SDS PAGE gel (Figure 5). The lanes are decoded in Table 9. Pure protein G (PG) was used as reference and two molecular weight ladders (L).

Table 9. Decodes Figure 5 by displaying what concentration of binding buffer is related to which well. L stands for the molecular weight ladder, E are empty lanes, the number for what concentration of the binding buffer, and PG for pure protein G stock.

Lane	**1**	**2**	**3**	**4**	**5**	**6**	**7**	**8**	**9**	**10**	**11**	**12**	**13**	**14**	**15**
Content	L	E	E	30	30	30	E	L	EE	-	20	20	20	-	PG

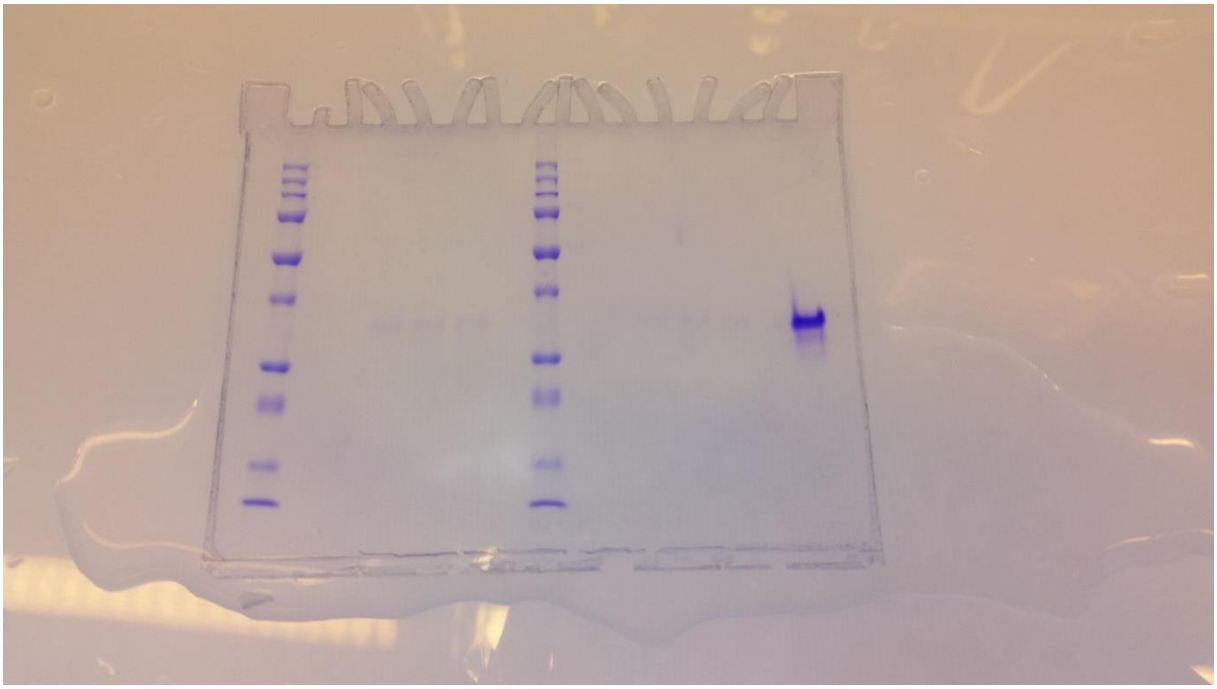

Figure 5. SDS-gel from binding study. Lanes are decoded in Table 9 and vague lines are observed for the binding buffer wells.

3.3 Cell Lysis

The results from the cell lysis for the ratio sample buffer: BBM at two different ratios (Table 10 and Table 11). Additionally, the ratio between the blanc using running buffer instead of sample and the reaction with sample is calculated. The greatest reduction for the [1:1] ratio is at 60 seconds (Table 10) and at 240 seconds (Table 11).

Table 10. Measured OD signal at 620 nm from the BBM and sample reactions. Two blanks: running buffer vs BBM and running buffer vs sample were also measured. A change in E.coli stock was performed at (*).

Ratio [1:1]	**0 [s]**	**30 [s]**	**60 [s]**	**120 [s]**	**240 [s]**
Running Buffer: BBM	0.030	0.033	0.030	0.018	0.022
Sample:Running Buffer	0.992	0.931	1.01 *	1.03	0.850
Sample: BBM	0.895	0.709	0.559	0.628	0.562
Ratio	0.902	0.762	0.552	0.611	0.661
Reduction [%]	-9.78	-23.8	-44.8	-38.9	-33.9

Table 11. The measured OD at 620 nm for the reactions of BBM with sample are displayed. Two blanks were performed using running buffer vs BBM and running buffer vs sample.

Ratio [1:2]	**0 [s]**	**30 [s]**	**60 [s]**	**120 [s]**	**240 [s]**
Running Buffer: BBM	0.15	0.093	-	-	-
Sample:Running Buffer	0.609	0.742	0.74*	0.653	0.619
Sample: BBM	0.567	0.563	0.299	0.3	0.247
Ratio	0.931	0.759	0.404	0.459	0.399
Reduction [%]	-6.90	-24.1	-59.6	-54.1	-60.1

3.4 Dilution Determination

The measured signals from the different volumes of *E.coli* re-arranged after size are documented in Table 12. For volume 80, one of the measurements was compromised by a bubble and therefore is not included. In the case of volume 40, only 5 measurements were taken. The *E.coli* stock had a signal of 0.401 after a times-20 dilution, recalculated.

Table 12. From the dilution determination the following signal were measured for the different E.coli volumes. In the cases where no measurements were done, the table is marked with and x.

Volume [µl]	**Signal 1 (620 nm)**	**Signal 2 (620 nm)**	**Signal 3 (620 nm)**	**Signal 4 (620 nm)**	**Signal 5 (620 nm)**	**Signal 6 (620 nm)**
80	0.343	0.375	0.379	0.41	0.456	x
40	0.351	0.371	0.398	0.43	0.458	x
20	0.249	0.265	0.287	0.294	0.336	0.402
10	0.118	0.211	0.240	0.255	0.261	0.273

The data was controlled for outliers prior to calculating the average (Table 13). Included in the Table is also the standard deviation and average for each volume set. A visual representation is displayed in Appendix K.

Table 13. Based on Table 12, the upper and lower limits were calculated to evaluate if gathered data contained outliers. Additionally, the standard deviation and signal average were calculated.

Volume [µl]	Q1	Q2	IQR	Lower Limit	Upper Limit	Standard Variation	Average
80	0.356	0.433	0.074	0.248	0.544	0.0427	0.393
40	0.361	0.444	0.083	0.237	0.569	0.0425	0.402
20	0.267	0.344	0.077	0.152	0.460	0.0558	0.306
10	0.190	0.263	0.073	0.080	0.373	0.0572	0.226

The dilutions of the system according to each average listed in Table 13. Table 14 also displays the calculated OD of each diluted injected sample, utilizing the measured OD of the *E.coli* stock.

Table 14. Lists the calculated dilutions from each E.coli sample volume.

Volume	Predicted OD of Injection Sample	Calculated system dilution
80	2.01	5.11
40	2.67	6.66
20	4.01	13.1
10	8.02	35.4

In Figure 6, the different dilutions from Table 14 are displayed. A power-curve was fitted to the results.

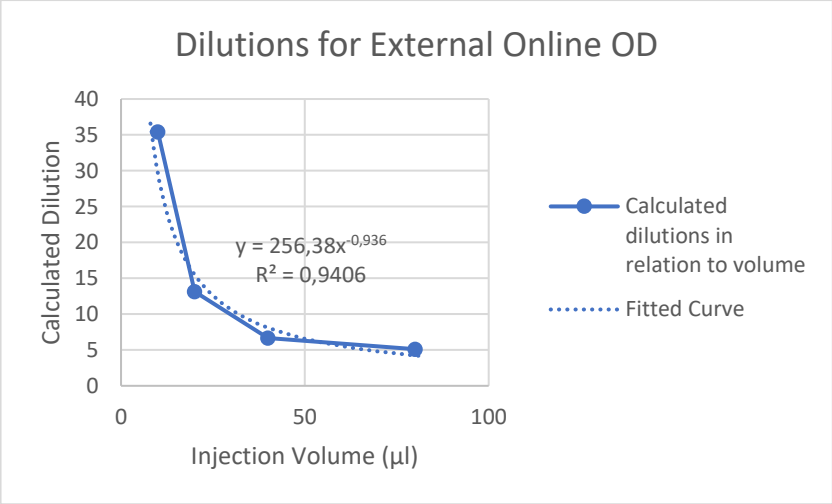

Figure 6. The plotted average dilutions versus the injection volume. A power-curve was fitted to the data.

3.5 Fermentation

3.5.1 Running Scheme

Observations of the systems robustness were made during the final fermentation. During the measurement of OD, the number of cycles at each volume (80, 40, 20 and 10) could be varied depending on the growth of the *E.coli*. The program was initially set to three cycles at 80 µl and six cycles at 40 µl. Following the growth, the robustness of the system was put to the test by variating four parameters to accommodate the fermentation: running buffer volume, number of cycles at set volume, the sample volume, and the time to dwell until the next hour. The three latter parameters were the parameters being observed.

It was observed that changes in the system during an active scheme did, to a large extent, not disturb the process. The only parameter that did no consistently update with the changes was the dwell function used to pause the sampling until the next hour.
The final resulting scheme used for the fermentations are described in Appendix C.

3.5.2 Internal OD Measurements vs External OD Measurements

An outtake of the times registered from the fermentation is listed in the Table 15 below. Smaller variations can occur depending on the volume sample used for the Measure OD step. Not included in Table 15 is the running time for initiation once and clean all inlet tubes.

Table 15. An example of the time required for each sample, the total time for one scheme and the time from start to recombinant protein recovery.

Sub-scheme	Initiation	Measure OD	Sampling, binding and elution	Cleaning	Pause To set loops	Summarized time per sampling moment [s]	Time product recover [s]
Time [s]	232	116	767	479	30	1 624 (27.07 minutes)	1115 (18.58 minutes)

The online measuring of OD was implemented with a fermentation. Using the calculated dilutions in Table 5 yielded the online external OD, which in combination with the offline OD are displayed in Figure 7. Another example of the growth curve from the online and offline measurements is displayed in Appendix D.

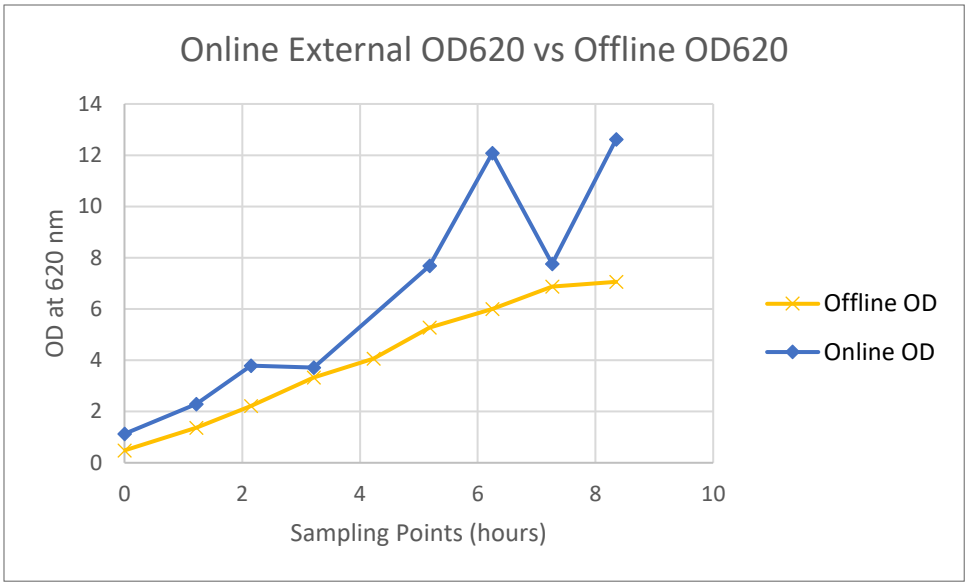

Figure 7. The online versus offline measured cell OD. Difference between the two could be due to air-bubbles at the end.

Figure 8 shows the offline OD measurements relative to the glucose concentration. The glucose level plateaus after 4 hours of fermentation which indicates the auto-induction. The retrieved data from the online and offline measurements regarding OD and glucose concentration can be found in Appendix L.

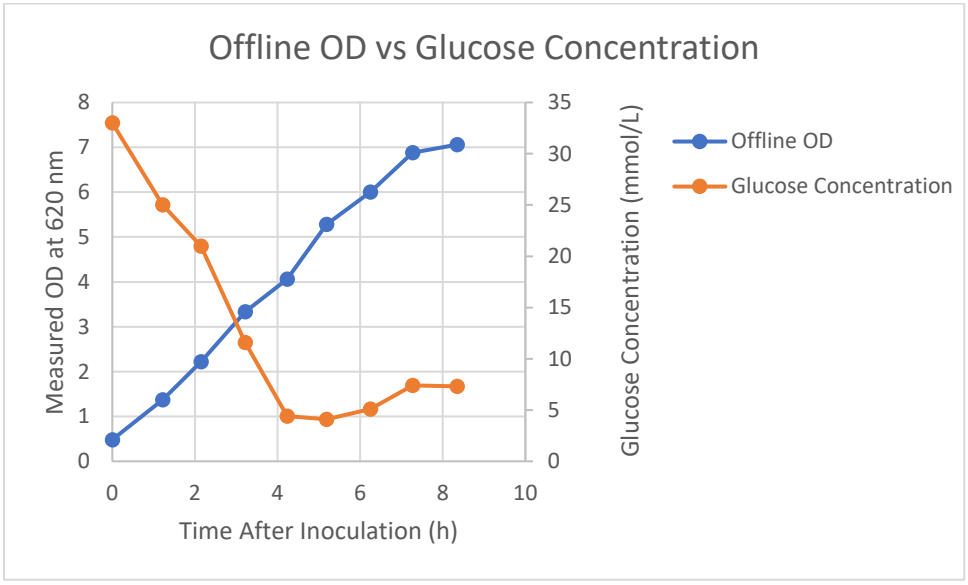

Figure 8. Offline cell OD versus glucose measurements. The glucose measurements increase slightly towards the end of the fermentation.

The SDS-gels for the offline sample and supernatant of the offline sample are displayed in Figure 9 below. Table 16 is used to decode the lanes of Figure 9. In Appendix G, the SDS-gel for the online sampling is displayed. No bands are seen for the online sample, whilst the offline samples contain bands on the same molecular weight as the pure protein G. The online ELISA is displayed in Appendix I, the results are inconclusive.

Table 16. The distribution of the samples (S) from the fermentation, pure protein G (PG) and the molecular weight (L) over the wells on the SDS-gel. Any empty lanes are marked with an (-).

Lane	**1**	**2**	**3**	**4**	**5**	**6**	**7**	**8**	**9**	**10**	**11**	**12**
Sample	PG	-	S 9	S 8	S 3	L	S 6	S 5	S 4	S 3	S 2	S 1

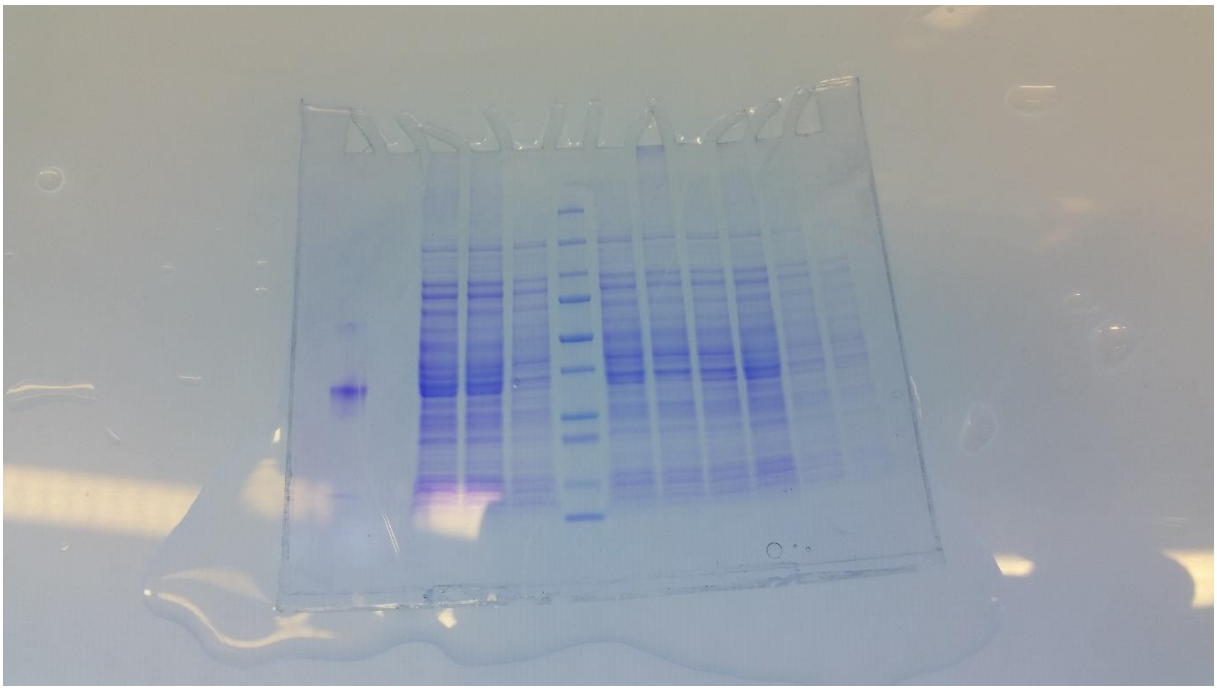

Figure 9. SDS-gel of the supernatant from the fermentation.

3.5.3 Internal UV-detector Internal Monitoring of the Fermentation

Figure 10 displays a figure from the online monitoring of the fermentation. The first increase in signal is the flow-through from the column during binding and elution. Following the flow-through are two defined elution peaks.

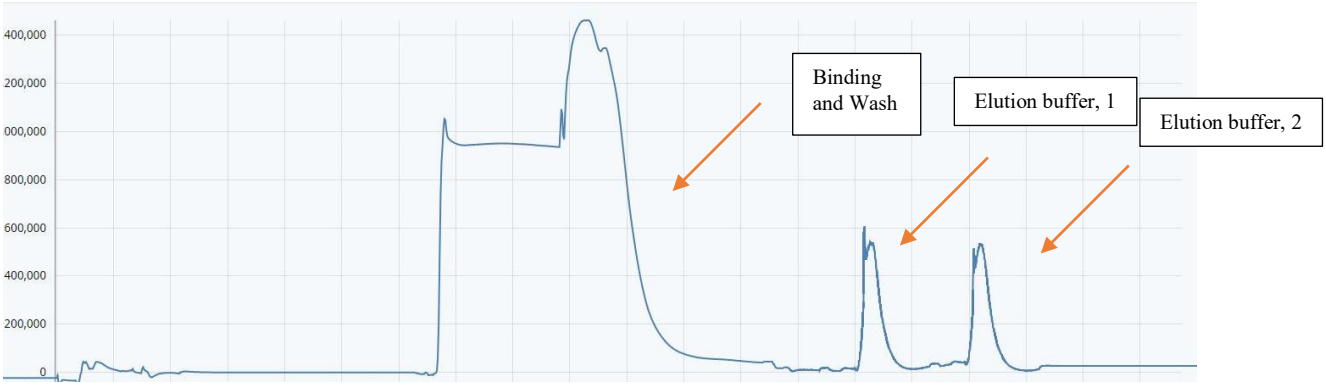

Figure 10. An example of the online monitoring using the Internal UV-detector. The figure includes binding and washing, and the two loops of elution.

3 Discussion

The sub-schemes described in the materials and methods can be combined in several different sequences to create longer and more complex schemes. One reason for the versatility of the four sub-schemes is that the different Tecan functions can be constructed as parameters. Thus, the end user can e.g. use the same sub-scheme to move Tecan 2 and 4 in one sequence of Direction of Movements (O or I) and another sequence to perform another task.

Another important step was the different studies performed on the system. The binding and elution of the His-tagged protein was verified in Figure 5. Vague bands from the 20 mM binding buffer and 30 mM binding buffer experiments indicate that both concentrations are viable for the purification step. To reduce the amount of unspecific binding the 30 mM binding buffer was therefore chosen to avoid false-positive or false-negative results when in the future implementing an analytical tool (e.g. capacitive biosensor).

Compared to the study of cell lysis, the binding study had a more statistical strength with triplicates at each concentration. Observing the signals of lysis in Tables 10 and 11, the reasoning is pure iterative and based on trends as each combination of ratio and time was performed once. For both ratios, the reduction was greater at a reaction time of 60, 120 and 240 seconds compared to 0 and 30 seconds. At ratio 1:1 (sample:BBM) the reduction in signal was greater for 60 seconds than 240 seconds, whilst at 1:2 (sample:BBM) the reduction was the greatest from 240 seconds. The difference could be due to the measurement method as the flow through the cuvette was 50 µl/s and the measurement interval 2 seconds. Since the measuring is not constant, the peak of sample zone could have been missed, which also is the motivation for the results being iterative.

However, during the final fermentation an error in the scheme affected the lysis. In the final run, the 30% of the BBM was not dispensed to the confluent point due to an error later discovered in the scheme. Instead, 30% of binding buffer was pulled in. Consequentially, the sample was initially mixed with 45 µl of binding buffer and then 105 µl of BBM (Appendix E). It is assumed that the lysis is similar to that of the 1:1 (sample:BBM) dilution for 120 seconds rather than the 1:2 (sample:BBM) dilution. Considering the sensitivity of the capacitive biosensor, it is concluded that the difference in lysis ratio is not too low for detection. An advantage of the unfortunate change is that more binding buffer is mixed with the supernatant and could possibly improve the binding of the protein.

The final fermentation does not contain a clarification step such as centrifugation lifted both in the introduction (1.3) and used during the offline cell lysis (2.4.2). Without the separation of soluble and insoluble fractions, the number of cellular components flowing through the purification column is increased. If there is an increased risk of clogging, blockage from binding sites, or unwanted non-specific binding, as a result of not incorporating a clarification step, would have to be further evaluated. In the case of non-specific binding, the binding study only examined the binding and elution of pure protein G. If other proteins contain histidine, then another concentration on the binding and washing buffer could be more optimal.

The effects of dispersions (Eq. 3) that were measured during the dilution determination (Table 12) was a step towards decoding the OD measurements from the fermentation. Due to the risk of inconsistencies in the measurements from the measuring interval, repeating the experiment at a minimum of five times narrowed the distance between the calculated dilution and the equivalent real OD. The difference between the online OD and offline OD from Figure 7 is therefore probably due to other factors. One such factor could be air-bubbles or other

particles disturbing the signal. From the figures in Appendix H, there baseline after the signal appears not to be constant. Therefore, there are indications that the difference is, to a great extent, due to disturbances rather than the approximations or measuring method.

An outtake from a previous fermentation (Appendix D), displays a greater correlation between offline and online measurements in terms of curvature. The difference in OD could be due to different sample volumes were used than in the dilution determination study. Therefore, the equation of the fitted exponentiation curve was used to translate the volumes into dilutions. Since the fitted curve is not completely optimized, the dilutions from Appendix D are approximative. Conclusively, the translation is adequate to see the trend in growth of the online samples but with a marginal difference in OD compared to the offline measurements.

The reason for the difference between Figure 7 and Appendix D could depend on the difference in tube size, flow of the uptake or pO_2 as these were the main differences between the two set-ups. A bigger tube diameter might make uptake of particles that disturb the external spectrophotometer more possible however this would need to be further studied before any conclusion can be drawn.

According to Equation 4 the connection of the sample plug and the BBM at the equal flow of 5 µl/s would theoretically have increased the dispersion by a factor of two. Thus, the functionality of the confluent point during fermentation was to increase the dispersion to ultimately increase the percentage of lysed cells. Additionally, the cells that did intertwine, from the final scheme, with the BBM at the confluent point could have undergone more lysis. From Appendix J, an estimation of the final eluted amount of protein G was calculated. However, this calculation only serves an iterative idea of what concentration range the protein might be in as it builds on several assumptions. The limitations to the analysis of that calculation lies in the difference of choice of media and induction mode. Nevertheless, if the protein G concentration is within a quite broad vicinity of the approximated calculation, the implementation of a capacitive biosensor would be able to detect the protein.

The online samples of purified protein G from the lysis was not detected on the SDS-gel (Appendix G), this could be due to the concentration being too low. The second attempt of analysing the online samples, the ELISA (Appendix I), did not show much change in signal. There could be several different reasons why the ELISA did not work. Either the protein concentrations were too low, no protein was sampled, the imidazole might have disturbed the interactions, cross-contamination, or the protein was not functional. From the offline SDS-gel (Figure 9), there appears a band at a similar molecular weight as the purified protein G. Additionally, the binding study verified that the protein in the purified form can be bound, eluted and sampled from the IMAC. Further investigations could be performed to determine if imidazole could affect the protein G – IgG interactions. Regarding the concentration, the implementation of a biosensor could verify if the protein is present and functional as the sensitivity of the analytical tool is high. Observing Figure 10 where the signal from the internal UV-detector is displayed, the curvature of the elution buffer is different than the signals displayed in Figure 1. The extra peaks observed could be due to protein G being eluted, however further experiments would have to be performed.

Though the lumen catheter has the advantage of avoiding vivid cells in the system, due to the intent of reducing the dead-volume the catheter was excluded from this study. The bottleneck of the design of this system is the handling of living cells. A few measurements were taken to reduce the extent of contamination. However, it should be emphasized that the optimal scenario would include a smaller design of a double lumen catheter. Steps taken to minimize accumulation of living cells in the system were to only use loop 2 after the lysis step. This loop

was purposely kept cell free so that cells left in the tubing leading from loop 1 to the confluent point does not contaminate the rest of the system. Additionally, the path from loop 1 and loop 2 leading past the online internal UV-detector were cleaned with ethanol in-between each sampling point. Finally, after the complete fermentation, all inlet tubes are rinsed with an ethanol pulse.

The incorporation of auto-induction into the online monitoring and sampling set-up reduces the amount of direct human interference with the reactor but is also cost efficient. As the set-up includes lower volume requirements to perform the same task (sampling, binding buffer and elution buffer compared to offline demands), a digitalized monitoring and documentation system for efficiency, and in theory an analytical tool (e.g. capacitive biosensor) for rapid analysis, another cost reductive step strengthens the advantages of atomizing more steps of a fermentation.

To relate to the directives of the Eudralex, specifically the criterium of the sample mimicking the reactor content, the connection to online sampling and monitoring systems is the analysis of the sample. Rapid information retrieval from the sample analysis, where the sample reflects the fermentation content, could potentially introduce more options of action. Therefore, developing online sampling techniques is of global industrial relevance as it has already been established through regulations by the European Commission that the information of the reactor content is important.

The relevance of online sampling and monitoring systems such as the VersAFlo are imperative. To sample and elute protein took less than 30 minutes (including cleaning) with the scheme in Appendix C. The time reduction from implementing an online monitoring system correlates to information obtained earlier of the status in the bioreactor. If a batch is not working or resulting in abnormal signals, the fermentation can be stopped at an early stage, in comparison to the hours an ELISA requires.

An additional advantage of using online sampling and monitoring systems is the robustness. The robustness of the scheme permits updates to the system during the fermentation to adapt to the process instead of losing information. An example of such a scenario was the dilution step prior to the online OD measurements, where the injection volume could be reduced to maintain a signal within the linear range. Additionally, the closer in time the results of the samples are to the current state of the content in the reactor, there is a possibility to develop and implement a feedback control system where the monitoring program stops the fermentation if the results differ greatly from the guidelines. Ultimately there is an economical benefit of obtaining the results within minutes instead of hours.

4 Conclusion

The versatility and robustness of the created online monitoring and sampling scheme opens the possibility of time reduction of the analysis and reduction in economic costs from failed fermentations. For pure his-tagged protein G, 30 mM binding buffer is recommended. By implementing an analytical tool such as the capacitive biosensor at the end of the sampling scheme, reduced consumption of chemicals, sample volumes and potential fast feedback can be achieved.

5 Future Aspects

The final scheme uses a low volume sample adapted for a sensitive final analytical tool such as a capacitive biosensor. Moving forward, a biosensor immobilized with IgG could be implemented to verify the protein production and purification for the entire system.

Future studies could involve the control of contamination after usage or implementing standards in accordance with the Eudralex. One improvement would be to implement a double-lumen catheter in the sampling step. However, the size of the catheter should be chosen to minimize any dead-volume as much as possible.

Further studies could be made by ELISA and the usage of a capacitive biosensor to determine if imidazole influences the results from the detection system. Regarding the tracking of cellular OD, a degasser should be implemented prior to the detection. The binding study could be broadened to incorporate the crude protein to see if the results would differ. Further volume optimization can also be performed to establish a balanced ratio between time, and sample and BugBuster® MasterMix volumes for cell lysis.

The robustness of the VersAFlo system indicates that other areas could be further studied and developed. The first possibility is the implementation of multi-analysis as the three-way valves permit separation of the final flow. Future research could include the implementation of both a capacitive biosensor and a flow-ELISA scheme. If a buffer exchange step is included, then the internal UV-detector could possibly give more accurate data about the purified protein as the imidazole currently appeared to have interfered with the signal.

To further the potential of the online sampling and monitoring schemes, if implementation of multi-analytical tools is applied, then the development of a response stage could be investigated. Should the signal differ from a set delta value, then the system notifies the abnormality, opening up time for pro-activity.

6 References

Ahlqvist, J., Dainiak, M., Kumar, A., Hörnsten, E., Galaev, I., & Mattiassion, B. (2006). Monitoring the production of inclusion bodies during fermentation and enzymer-linked immunosorbent assay analysis of intact inclusion bodies using cryogel minicolumn plates. *Analytical biochemistry,* 345(2), 229-237. https://doi.org/10.1016/j.ab.2006.03.050

Bentley, W., Mirjalili, N., ANdersen, D., Davis, R., & Kompala, D. (1990). Plasmid-encoded protein: the prinicipal factor in the "metabolic burden" associated with recombinant bacteria. *Biotechnology and bioengineering*, 35(7), 668-681. https://doi.org/10.1002/bit.260350704

BIO RAD. (n.d. -a) *Transfer Buffer Formulations* [PDF file]. Retrieved August 17, 2018, from http://www.bio-rad.com/webroot/web/pdf/lsr/literature/Bulletin_6211.pdf

BIO RAD. (n.d. -b), *Protocol: Direct ELISA with streptavidin-biotin detection,* Retrieved August 17, 2018, from https://www.bio-rad-antibodies.com/direct-elisa-protocol-with-streptavidin-biotin-detection.html

Bird, R.B, Steward, W.E., Lightfoot, E.D. (2006), Transport Phenomena (Revised 2nd Edition ed.). John Wiley & Sons Ltd. Retrieved August 12, 2018, from https://www.slideshare.net/Aapandove/bird-stewart-lightfoot-2002-transport-phenomena-2nd-ed

Collins, A., Nandakumar, M., Csöregi, E. & Mattiassion, B. (2001). Monitoring of a-ketoglutarate in a fermentation process using expanded bed enzyme reactors. *Biosensors and Bioelectronics*, 16(9-12), 765-771. https://doi.org/10.1016/S0956-5663(01)00218-4

Crowe, J., Dobeli, H., Gentz, R., Hochuli, E., Stiiber, D., & Henco, K. (1994). 6xffis-ni-nta chromatography as a superior technique in recombinant protein expression/purification. In *Protocols for gene analysis* (pp. 371-387). Humana Press. https://doi.org/10.1385/0-89603-258-2:371

CUSABIO. (n.d.), *Direct ELISA Protocol* [PDF file]. Retrieved September 27, 2018, from http://www.cusabio.cn/ktsms/Direct_ELISA_Protocol.pdf

Dabros, M., Schuler, M., & Marison, I. (2010). Simple control of specific growth rate in biotechnological fed-betch processes based on enhanced online measurements of biomass. *Bioprocess and biosystems engineering*, 33(9), 1109-1118. https://doi.org/10.1007/s00449-010-0438-2

Erlandsson, D., Teeparuksapun, K., Mattiasson, B., & Hedström, M. (2014). Automated flow-injection immunosensor based on current pulse capacitive measurements. *Sensors and Actuators B: Chemical*, 190, 295-304. https://doi.org/10.1016/j.snb.2013.08.076

Ertürk, G., Hedström, M., Mattiasson, B., Ruzgas, T., & Lood, R. (2018). Highly sensitive detection and quantification of the secreted bacterial benevolence factor RoxP using a capacitive biosensor: A possible early detection system of oxidative skin disease. *PloS one,*

13(3), e0193754. doi:10.1371/journal.pone.0193754

European Commission Health and Consumers Directorate-General. (2011, February 7). *ec.europa.eu.* Retrieved August 16, 2018, from https://ec.europa.eu/health/sites/health/files/files/eudralex/vol-4/2011_intro_en.pdf

European Commission Health and Consumers Directorate-General. (2014, March28). *European Commission.* Retrieved August 16, 2018, from https://ec.europa.eu/health/sites/health/files/files/eudralex/vol-4/2014-11_vol4_chapter_6.pdf

Fling, S.P., Gregerson, D.S. (1986). Peptide and protein molecular weight determination by electrophoresis using a high-molarity tris buffer system without urea. *Analytical biochemistry,* 155(1), 83-88. https://doi.org/10.1016/0003-2697(86)90228-9

GE Healthcare. (n.d.). *Instructions 71-5027-68 AF*. Retrieved August 18, 2018, from https://www.auburn.edu/~duinedu/manuals/HisTrapHP.pdf

Glifberg, D., & Svensson T. (2016). Development of an online bioanalytical system. Unpublished report, Lund University, Lund.

Hoffman, B., Broadwater, J., Johnson, P., Harper. J., Fox, B., & Kenearly, W. (1995). Lactose fed-batch overexpression of recombinant metalloproteins in Escherichia coli BL21 (DE3): process control yielding high levels of metal-incorporated, soluble protein. *Protein expression and purification*, 6(5), 646-654. https://doi.org/10.1006/prep.1995.1085

Holst, O., Wennerberg C., Nordberg Karlsson, E. (n.d.), Batch Cultivation of Genetically Engineered Escherichia coli for Recombinant Protein Produciton, KBT115 Practical in Bioprocess Technology [Laboratory manual]. Lund: Lund University, Bioprocessteknik KBT115

Jenkins, W. (2004). Tracers of ocean mixing. In H. Holland, K. Turekian, & H. Elderfield (Eds.), The Oceans and Marine Geochemistry (6 ed., pp 226). Oxford, UK:Elsevier. Retrieved August 17, 2018, from https://books.google.se/books?hl=en&lr=&id=BnZ77tb18UEC&oi=fnd&pg=PA223&dq=Jenkins,+W.+J.+(2006).+Tracers+of+ocean+mixing.+The+Oceans+and+Marine+Geochemistry,+6,+223&ots=NM-ZytVhQP&sig=wNAM20sBho2xhsRQAeWN-bTNw4U&redir_esc=y#v=onepage&q=peclet&f=false

Kumar, M., Thakur, M., Senthuran, A., Senthuran, A., Karanth, N., Hatti-Kaul, R., & Mattiasson, B. (2001). An automated flow injection analysis system for on-line monitoring of glucose and L-lactate during lactic acid fermentation in a recycle bioreaction. *World Journal of Microbiology and Biotechnology*, 17(1), 23-29. https://doi.org/10.1023/A:1016699701903

Kumar, M., Mazlomi, M., Hedström, M., & Mattiasson, B. (2012). Versatile automated continuous flow system (VersAFlo) for bioanalysis and bioprocess control. *Sensors and Actuators B,* 161(1), 855-861. https://doi.org/10.1016/j.snb.2011.11.049

Laemmli, UK (1970), Cleavage of structural proteins during the assembly of the head of bacteriophage T4. *Nature* 227, 6680 -185. https://doi.org/10.1038/227680a0

Listwan, P., Pédelacq, J., Lockard, M., Bell, C., Terwilliger, T., & Waldo, G. (2010) The optimiation of in vitro high-throughput chemical lysis of Escherichia coli. Application to ACP domain of the polyketide synthase ppsC from Mycobacterium tuberculosis. *Journal of structural and functional genomics*, 11(1), 41-49. https://doi.org/10.1007/s10969-009-9077-8

Lu, Y., Peterson, J., Gooding, J., & Lee, N. (2012). Development of sensitive direct and indirect enzyme-linked immunosorbet assays (ELISAs) for monitoring bisphenol-A in canned foods and beverages. *Analytical and bioanalytical chemistry*, 403(6), 1607-1618. https://doi.org/10.1007/s00216-012-5969-8

Luo, Y.Z., & Pawliszyn, K. (2000). Membrane Extraction with a Sorbent Interface for Headspace Monitoring and Aqueous Samples using a Cap Sampling Device. *Analytical Chemsitry*, 72(5), 1058-1063. doi: 10.1021/ac990747b

Mazlomi, M., Hedström, M., & Mattiasson, B. (2010). Integrated set-up of sampling, sample treatment and assay of an integrated protein during fermentation. *Journal of biotechnology*, 150(3), 366-371. https://doi.org/10.1016/j.jbiotec.2010.09.937

McKelvie, I. (2008), Principles of flow injection analysis. In *Comprehensive Analytical Chemistry* (Vol. 54, pp. 81-109). Elsevier. https://doi.org/10.1016/S0166-526X(08)00604-1

Mörtstedt, S., & Hellsten, G. (1987). *Data och Diagram* (76 ed.). Stockholm: Esselte studium.

Nilsson, M., Vijayakumar, A., Holst, O., Schornack, C., Håksanson, H., & Mattiasson, B. (1994). On-line monitoring of product concentration by flow-ELISA in an integrated fermentation and purification process. *Journal of fermentation and bioengineering*, 78(5), 356-360.

Nilsson, M., Håkansson, H. & Mattiasson, B. (1992). Process monitoring by flow-injection immunoassay: Evaluation of a sequential competitive binding assay. *Journal of Chromatography A*, 597(1-2), 383-389. https://doi.org/10.1016/0021-9673(92)80135-H

Nouri, A., Ahari, H., & Shahbazzadeh, D. (2018). Designing a direct ELISA kit for the detection of Staphylococcus aureus enterotoxin A in raw milke samples. *International journal of biological macromolecules*, 107(Part B), 1732-1737. https://doi.org/10.1016/j.ijbiomac.2017.10.052

Merck. (n.d.) *BugBuster® Protein Extraction Reagent*. Retrieved August 17, from http://www.merckmillipore.com/SE/en/product/BugBuster-Master-Mix,EMD_BIO-71456#anchor_USP

Patil, R. H., Nadar, M. D., & Ali, R. (2017). The influence of Dean Number on heat transfer to Newtonian fluid through spiral coils with constant wall temperature in laminar flow. *Heat and Mass Transfer*, 53(5), 1843-1850. https://doi.org/10.1007/s00231-016-1937-8

Picque, D., & Corrieu, G. (1992). Performances of aseptic sampling devices for on-line monitoring of fermentation processes. *Biotechnology and bioengineering*, 40(8), 919-924. https://doi.org/10.1002/bit.260400808

Riesenberg, D., Schulz, V., Knorre, W. A., Pohl, H. D., Korz, D., Sanders, E. A., Roß, A., & Deckwer, W. D. (1991). High cell density cultivation of Escherichia coli at controlled specific growth rate. *Journal of biotechnology*, 20(1), 17-27. https://doi.org/10.1016/0168-1656(91)90032-Q

Růžička, J., & Hansen, E. H. (1978). Flow injection analysis: Part X. theory, techniques and trends. *Analytica Chimica Acta*, 99(1), 37-76. https://doi.org/10.1016/S0003-2670(01)84498-6

Schmitt, J., Hess, H., & Stunnenberg, H. G. (1993). Affinity purification of histidine-tagged proteins. *Molecular biology reports*, 18(3), 223-230. https://doi.org/10.1007/BF01674434

Sezonov, G., Joseleau-Petit, D., & D'Ari, R. (2007). Escherichia coli physiology in Luria-Bertani broth. *Journal of bacteriology*, 189(23), 8746-8749. DOI: 10.1128/JB.01368-07

Spencer, K., Cowans, N. J., & Nicolaides, K. H. (2008). Maternal serum inhibin-A and activin-A levels in the first trimester of pregnancies developing pre-eclampsia. *Ultrasound in Obstetrics and Gynecology: The Official Journal of the International Society of Ultrasound in Obstetrics and Gynecology*, 32(5), 622-626. https://doi.org/10.1002/uog.6212

Squires, T. M., & Quake, S. R. (2005). Microfluidics: Fluid physics at the nanoliter scale. *Reviews of modern physics*, 77(3), 977. https://doi.org/10.1103/RevModPhys.77.977

Studier, F. W. (2005). Protein production by auto-induction in high-density shaking cultures. *Protein expression and purification*, 41(1), 207-234. https://doi.org/10.1016/j.pep.2005.01.016

Teeparuksapun, K., Hedström, M., Kanatharana, P., Thavarungkul, P., & Mattiasson, B. (2012). Capacitive immunosensor for the detection of host cell proteins. *Journal of biotechnology*, 157(1), 207-213. https://doi.org/10.1016/j.jbiotec.2011.11.004

Thermofisher (n.d.). Pierce™ Recombinant Protein G. Retrieved August 18 , 2018, from https://www.thermofisher.com/order/catalog/product/21193

U.S. Food and Drug Administration. (2004, September). Guidance for Industry PAT – A Framework for Innovative Pharmaceutical Development Manufacturing, and Quality Assurance. Retrieved August 16, 2018, from https://www.fda.gov/downloads/drugs/guidances/ucm070305.pdf

Villadsen, J., Nielse, J., & Lidén, G. (2011), List of Symbols. In *Bioreaction Engineering* Principles (3rd Ed.) (pp. xiii - xix). Boston, MA: Springer. doi:10.1007/978-1-4419-9688-6

Villadsen, J., Nielse, J., & Lidén, G. (2011), Chapter 10 Gas-Liquid Mass Transfer. In *Bioreaction Engineering Principles* (3rd Ed.) (pp. 459 - 496). Boston, MA: Springer. doi:10.1007/978-1-4419-9688-6

Wingfield, P. T. (2014). Preparation of Soluble Proteins from *Escherichia coli*. *Current*

Protocols in Protein Science, 78(1). https://doi.org/10.1002/0471140864.ps0602s78

Zhang, H., Yang, J., Yang, G., Want, X., & Fan, H. (2015). Production of recombinant protein G through high-density fermentation of engineered bacteria as well as purification. *Molecular medicine reports*, 12(2), 3132-3138. https://doi.org/10.3892/mmr.2015.3688

Appendix

Appendix A

A few general schemes that often are used are listed below. The schemes use the building blocks listed in the Table 2. The first few blocks are inspired by the sub-schemes previously developed by the CapSenze developers.

Fill Pump_ChangePort_EmptyLoop (FCE)
The first sub-schedule referred to in the methods is the FillPump_ChangePort_EmptyLoop (FCE) program.(Figure A1). With this program each step uses the same pump and valve to fulfil the commands. Some of the parameters are already set to fixed values or commands, whilst others can be changed depending on the scenario. An example of when this sub-schedule is used is to rinse the pump and loops (RinseLoops) which is displayed in Appendix C.

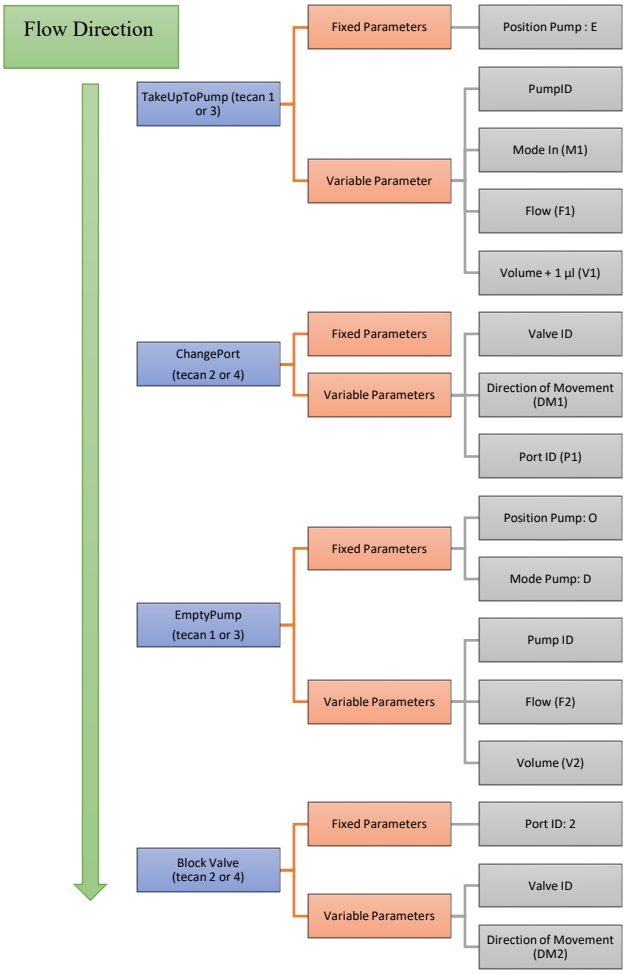

Figure A1. An illustrative description of the content of sub-scheme FCE. The scheme uses Tecan as building blocks and has fixed parameters and variable parameters.

TakeUpToPump_TakeUpFromY_SendToX_Sequence (TTSSe)

The TakeUpToPump_TakeUpFromY_SendToX_Sequence (TTSSe) scheme uses Tecan as building blocks and has fixed parameters and variable parameters (Figure A2). First the pump pulls in the running buffer or water in order to transport a sample zone over a longer distance. The designated valve then changes port and pulls in the desired volume of sample or solution at the set flow. Sequentially, the valve changes to the out-going port and sends the liquids in the pump and loop through the out-port. Finally, the valve changes port to the default blocking port. An example of when this sub-scheme is implemented during the measurements of cellular OD where the pump is prepared with running buffer, a sample plug pulled in, and the entire liquid sent through the external spectrophotometer.

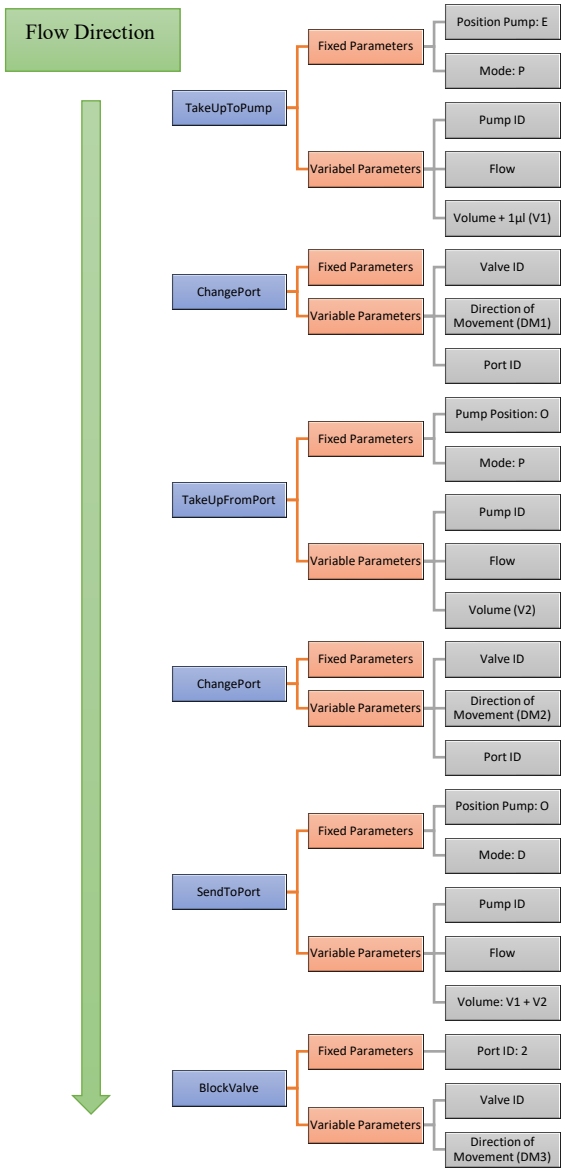

Figure A2. A flow-chart of the sub-scheme TTSSe. Fixed parameters and variable parameters are displayed.

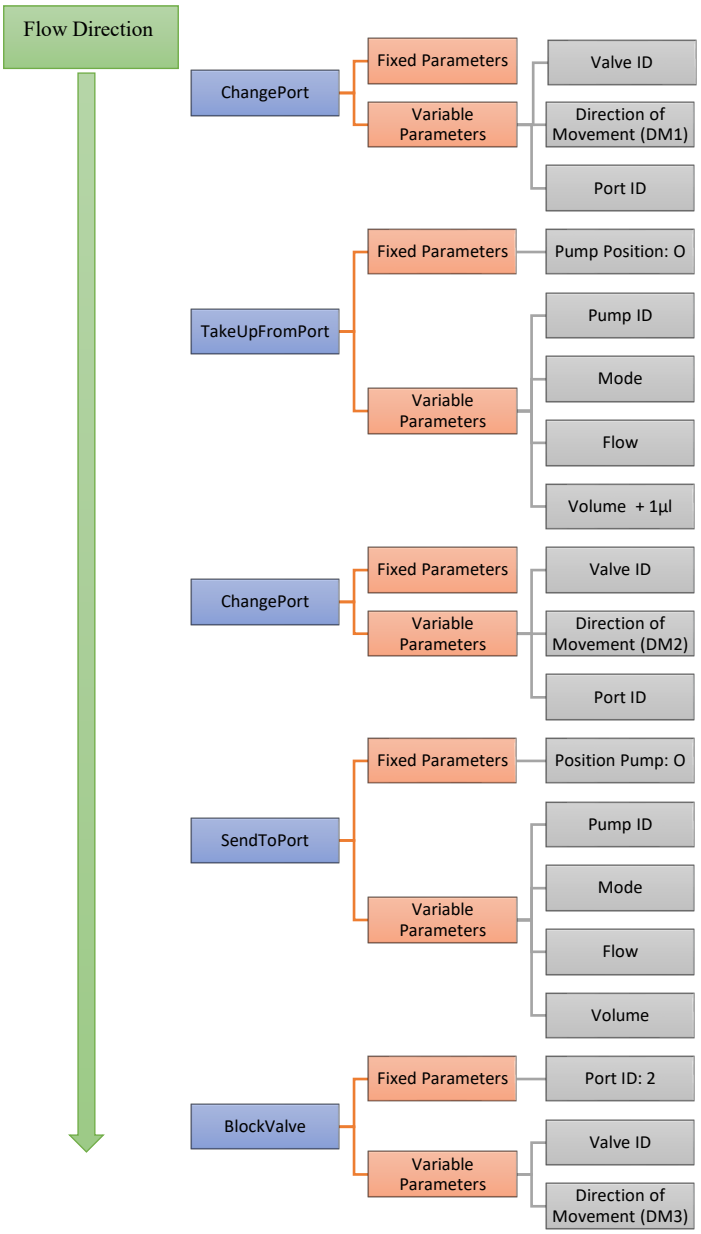

Figure A3. Displays the flow-chart for TSSe, including fixed parameters and variable parameters. The variable parameters can be changed depending on functionality.

TakeUpFromY_SentToX_Sequence (TSSe)

Similar to TTSSe, TakeUpFromY_ SendToX_ Sequence (TSSe) takes up from one port and sends to another (Figure A3). There is no priming of the loops with running buffer prior to taking up the liquid of interest. The active valve changes in the commanded direction to the designated port and uses the activated pump to take up (P or A) the set amount of volume with the set flow rate. Afterwards, the valve moves in the commanded direction to the out-port (port of choice) and sends the set volume through that port at the desired flow rate. The sub-scheme has port 2 as the default blocking port. This sub-scheme is active during the washing step after protein binding (Appendix C).

ValveAndPump_Sequence (VPSe)

The ValveAndPump_Sequence (VPSe) is used when a volume is to be injected into the loop and held there, or, a volume already injected into the loop is sent to another port (Figure A4). The active valve changes direction to the designated inlet or outlet port and uses the set pump to either take up (P or A) or send out (D or A) the desired volume at the set flow rate. This sub-schedule is active when the sample and BBM tubes are prepared for cell lysis. A sample plug is first pulled in from port 1 using the first pump and valve (Tecan units 1 and 2), and held there until lysis is to occur (Appendix C).

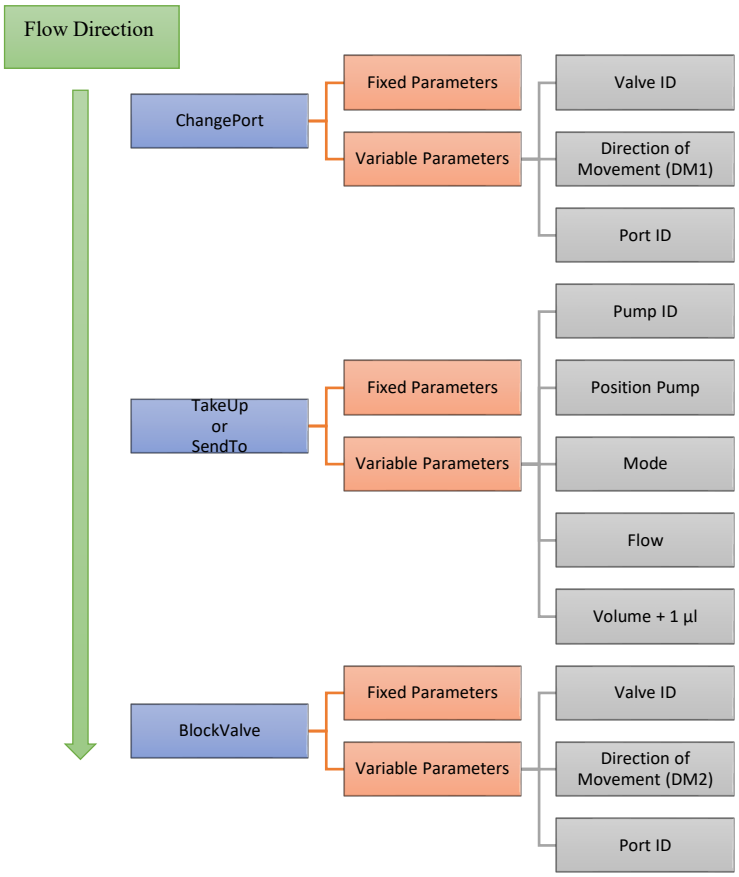

Figure A4. Flow schedule for VPS with fixed parameters and variable parameters. The schedule uses first the valve and then the pump to perform the task.

Appendix B

The four sub-schemes presented above are used to create larger schemes for more complex purposes. Below are examples of the larger sub-schemes used to create the final monitoring scheme. These schemes utilize other characteristics of the VersAFlo system such as Dwell, Internal UV-detector, Degasser. A flow-scheme for the entire sampling, binding and elution of protein is displayed below (Figure B1 to B3). This scheme was used for the last 7 sampling hours of the final fermentation. Prior to scheme, a description of each scheme used in the final run is described.

* It is advised that this parameter be set to D in future schemes.

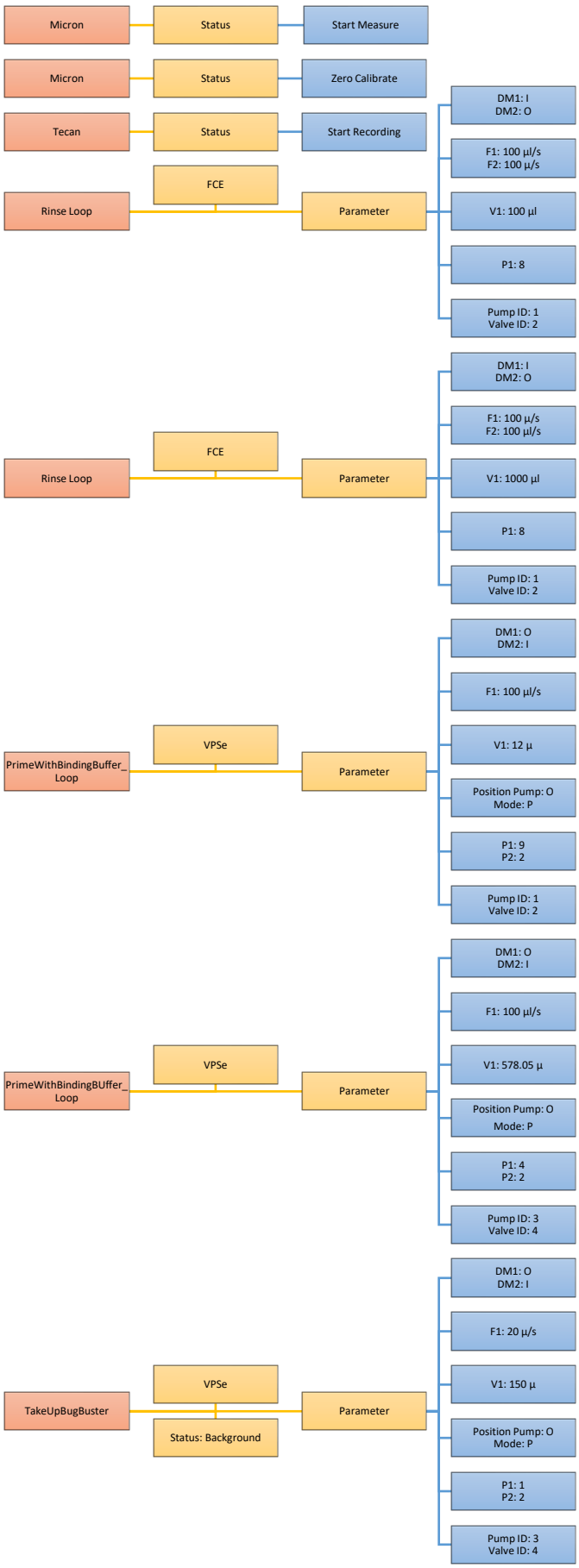

Figure B1. Part 1 of 3 for a scheme handling sampling, binding and elution.

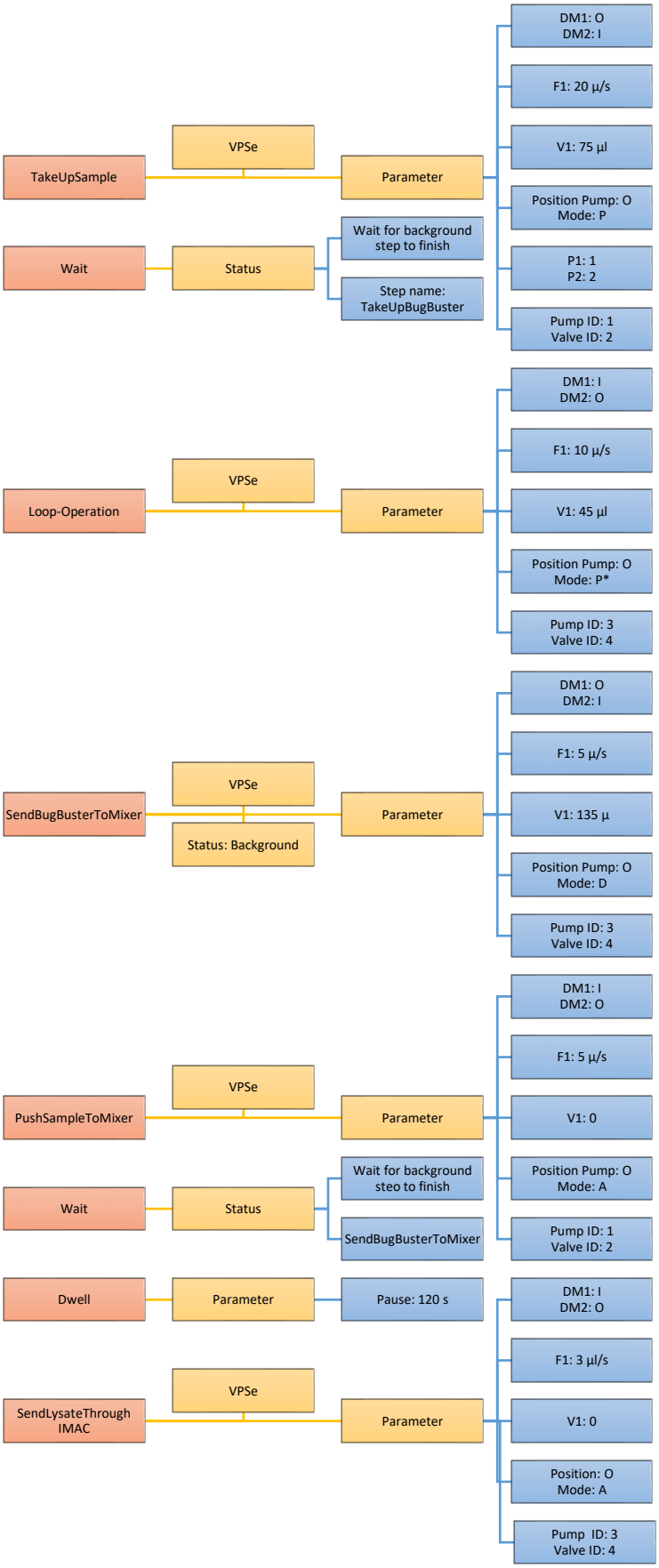

Figure B1 Part 2 of 3 for a scheme handling sampling, binding and elution.

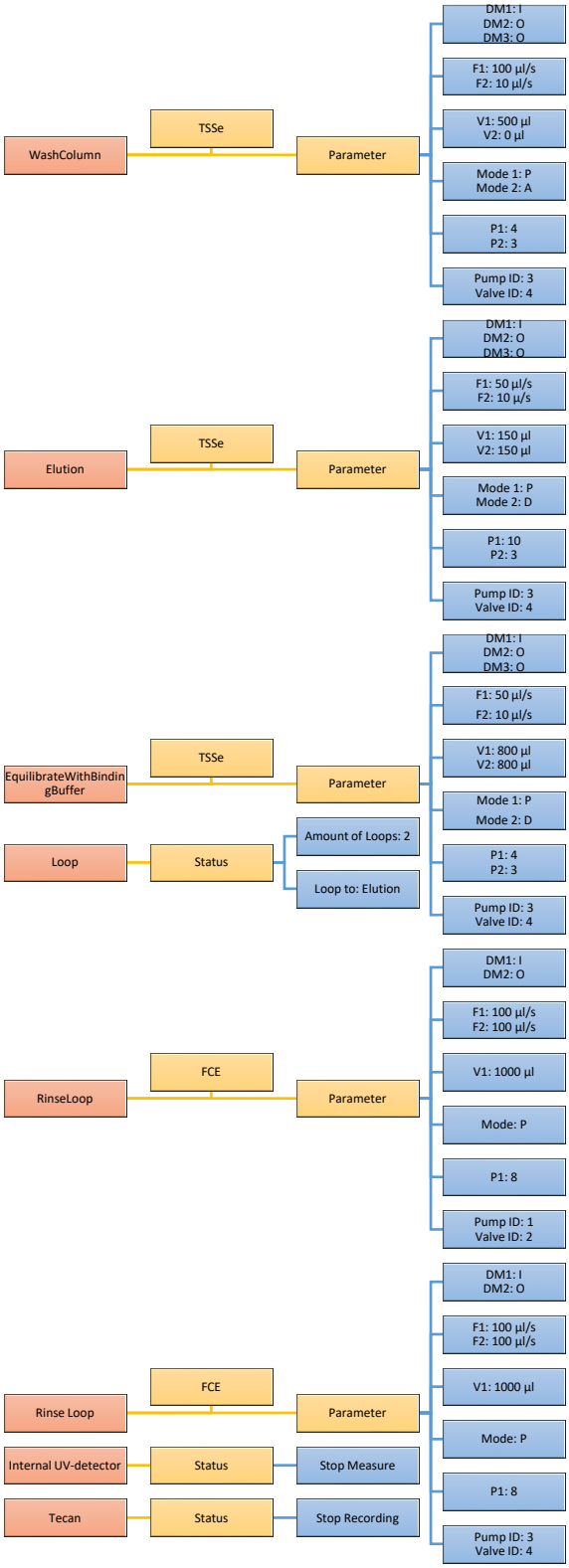

Figure B2. Part 3 of 3 for a scheme handling sampling, binding and elution.

Appendix C

Initiation Once

Commences with activating the degasser (GPIO). The lamp of the Micron 31 is turned on, the Micron 31 cleared and starts measuring. Following the Internal UV-detector preparation, the Tecan's recording is cleared and the actuator starts recording. The two loops are rinsed with running buffer (FCE) in both cases, 2000 µl running buffer is pulled in with a flow rate of 100 µl/s. The valve changes direction to the waste port (port 8) and empties the loop at a flow rate of 100 µl/s.

After rinsing both pumps and valves, the inlets tubes (except the sample tube) are primed. All priming tubes uses TTSSe. The parameters for each tube are summarized in Table C1. Directions are excluded.

Table C1. Parameters used for the initiation once prior to the fermentation run. The TTSSe sub-scheme (Appendix A) is activated where decoding the parameters can be performed.

Tube	Pump ID	Valve ID	P1	P2	F1 [µl/s]	F2 [µl/s]	F3 [µl/s]	V1 [µl]	V2 [µl]
BBM	3	4	1	8	50	20	50	400	86.9
Elution Buffer	3	4	10	8	100	100	100	400	114.1
Binding Buffer	3	4	4	8	100	100	100	400	321
Binding Buffer	1	2	9	8	100	100	100	400	127.1
Ethanol	1	2	12	8	100	100	100	400	348.2
Ethanol	3	4	12	8	100	100	100	400	195

After priming, the external spectrophotometer and the VersAFlo system is cleaned with 70% ethanol. In the latter case, first loop 1 through the Micron 31 is cleaned, then from port 7 of loop 2 and finally, after activating the third three-way valve, loop 2 via the IMAC. After cleaning, the third three-way valve is deactivated (Table C2).

Table C2. Cleaning of the VersAFlo system using 70% ethanol. All ports that lead to the Internal UV-detector from Tecan 2 or Tecan 4, and the spectrophotometer for OD measurements at 620 nm are cleaned.

Connection	Pump ID	Valve ID	P1	P2	F1 [µl/s]	F2 [µl/s]	F3 [µl/s]	V1 [µl]	V2 [µl]
Spectrophotometer	1	2	12	4	100	100	100	500	2500
Loop 1 via IMAC	1	2	12	3	100	100	10	400	1000
Loop 2 via port 7	3	4	12	7	100	50	10	50	300
Loop 2 via IMAC	3	4	12	3	100	100	10	400	1000

In order to evaluate if there are any air bubbles in the system that could disturb the Internal UV-detector, running buffer is pumped from Tecan 1 and Tecan 3. Sub-scheme FCE is active in both cases (Table C3).

Table C3. The parameters used to control if there are any air-bubbles in the system are listed. FCE is active.

Connection	Pump ID	Valve ID	P1	F1 [µl/s]	F2 [µl/s]	V1 [µl]
Loop 1 via IMAC	1	2	3	100	10	1000
Loop 2 via IMAC	3	4	3	100	10	1000
Loop 2 via port 7	3	4	7	100	10	1000

The Internal UV-detector is zero calibrated, the Dwell function activated for 20 seconds so that the user can check for bubbles and update the amount of loops. The number of loops was set to 2 and the program would repeat the sub-schemes from CheckForBubbles from loop 1. From loop 2 via port 7, the system is checked for bubbles, the system paused for 20 seconds (Dwell) and the loop function set to 2 where the system loops back to CheckForBubbles from loop 2 via port 7. Finally, the Internal UV-detector and the Tecan stop recording.

Initiation

The purpose of the initiation scheme is to equilibrate the system with binding buffer (using TSSe) and prime the sample tube (TTSSe). First the Internal UV-detector and Tecan start recording. The first and second loop are rinsed with running buffer using FCE (Table C4). All ports leading to the Internal UV-detector (Tecan 2 port 3, Tecan 4 port3, and Tecan 4 port 7) are equilibrated with binding buffer (TSSe) (Table C5), and the Internal UV-detector is zero calibrated. Finally, the sample tube is primed using the TTSSe sub-scheme (Table C6), the Internal UV-detector stops measuring and the Tecan stops recording.

Table C4. The necessary parameters to rinse the first and second loop using the combination of Tecan 1 and 2 or Tecan 3 and 4 are displayed.

Loop	Pump ID	Valve ID	P1	DM1	DM2	Mode 1	F1 [µl/s]	F2 [µl/s]	V1 [µl]
1	1	2	8	I	O	P	100	100	1000
2	3	4	8	I	O	P	100	100	1000

Table C5. Displays the parameters needed to equilibrate the affinity column and zero calibrate the Internal UV-detector are listed. Under loop, the pathways taken for equilibration are indicated

Loop	Pump ID	Valve ID	P1	P2	DM1	DM2	DM3	Mode 1	Mode 2	F1 [µl/s]	F2 [µl/s]	V1 [µl]	Vs [µl]
Loop 2, Port 7	3	4	4	7	I	I	O	P	D	20	10	50	50
Loop 1	1	2	9	3	I	O	O	P	A	50	10	500	0
Loop 2	3	4	4	3	I	O	O	P	A	100	10	500	0

Table C6. Prime sample tubes parameters.

Loop	Pump ID	Valve ID	P1	P2	DM1	DM2	DM3	F1 [µl/s]	F2 [µl/s]	F3 [µl/s]	V1 [µl]	V2 [µl]
1	1	2	1	8	O	I	O	100	50	100	550	1000

Measure OD

The Measure OD scheme is used for the online OD measurements at 620 nm. The parameters that vary are the volume of the sample plug and the volume of the running buffer behind the sample zone. First the Tecan starts recording and the first loop is rinsed using FCE (Table C7). Secondly, TTSSe is activated and running buffer is taken up followed by the sample plug. Table C8 displays the general settings of the parameters whilst Table C9 lists the sample volumes and equivalent running buffer volumes. Finally, the Tecan stops recording.

Table C7. The needed parameters to rinse the first loop using Tecan 1 and 2 are listed.

Loop	Pump ID	Valve ID	P1	DM1	DM2	F1 [µl/s]	F2 [µl/s]	V1 [µl]
1	1	2	8	I	O	100	100	1000

Table C8. The commands for the parameters used for the uptake of the sample plug and transportation to the spectrophotometer are listed.

Loop	Pump ID	Valve ID	P1	P2	DM1	DM2	DM3	F1 [µl/s]	F2 [µl/s]	F3 [µl/s]
1	1	2	1	4	O	I	O	100	20	50

Table C9. The different volumes of the sample plug measured and the volume running buffer following the sample zone are displayed.

Volume Sample [µl]	80	40	20	10
Volume Running Buffer [µl]	2720	2460	2780	2790

Sampling and Elution

The Sampling and Elution scheme is used for sample preparation. Where a sample plug is mixed with BBM and the His-tagged protein bound to the IMAC followed by elution. During the first three sampling moments the two elution plugs were combined to a bigger elution buffer plug and the column instead washed with an extra amount of binding buffer. This combination was later updated during the run so that two elution peaks intermediated by binding buffer was performed. The detailed flow-scheme for the later update is displayed in Appendix B and won't be further described here.

Cleaning

The cleaning schedule begins with the Tecan starting to record and the Internal UV-detector checks so that the lamp is on. Loop 1 and 2 are rinsed according to Table C10, the spectrophotometer, the system via loop 1, loop 2 and loop 2 (port 7) are cleaned using TTSSe and 70% ethanol (Table C11). Before loop 2 (port 7) the third three-way valve is activated. The Tecan stops recording and the Internal UV-detector stops measuring.

Table C10. Rinse loops.

Loop	Pump ID	Valve ID	P1	DM1	DM2	Mode 1	F1 [µl/s]	F2 [µl/s]	V1 [µl]	V2 [µl]
1	1	2	8	I	O	P	100	100	1000	1000
2	3	4	8	I	O	P	100	100	1000	1000

Table C11. Clean system. Spec stands for spectrophotometer,

Connection	Pump ID	Valve ID	P1	P2	DM1	DM2	DM3	F1 [µl/s]	F2 [µl/s]	F3 [µl/s]	V1 [µl]	V2 [µl]
Spec	1	2	12	4	I	O	O	100	100	100	500	2500
Loop 1 via IMAC	1	2	12	3	I	O	O	100	50	10	400	1000
Loop 2 via IMAC	3	4	12	3	I	O	O	100	100	10	500	1500
Loop 2 via port 7	3	4	12	7	I	O	O	100	50	10	250	500

PauseToSetTime

The parameter that can be changed here is the number of seconds that the Dwell function is active. By pausing the system for 30 seconds, the user can update the Dwell time until the next sampling hour.

PauseUntilNextHour

As mentioned above, the system pauses (Dwell) until the next sampling hour. The variation depends on the sample volume injected during Measure OD.

Loop

The loop function starts another cycle of measurements by looping back to the Initiation step. The number of loops is set as a parameter so that the user can update the number of cycles if needed.

CleanAllInTubes

This scheme is manually activated after the last run. It cleans all inlet tubes with 70% ethanol except for the ethanol tube. All of the tubes cleaned use the TTSSe scheme (Table C12).

Table C12. Cleans all in tubes.

Tube	Pump ID	Valve ID	P1	P2	DM1	DM2	DM3	F1 [µl/s]	F2 [µl/s]	F3 [µl/s]	V1 [µl]	V2 [µl]
EtOH	1	2	12	8	I	O	O	100	100	100	500	500
EtOH	3	4	12	8	I	O	O	100	100	100	500	500
Sample	1	2	12	1	I	O	I	100	100	100	300	1000
BBM	3	4	12	1	I	O	I	100	100	100	100	500
Binding Buffer	1	2	12	9	I	O	O	100	100	100	200	500
Binding Buffer	3	4	12	4	I	O	O	100	100	100	200	200
Elution Buffer	3	4	12	10	I	O	O	100	100	100	100	400

Combining the Schemes

During the final fermentation the following schemes and function were combined to create a full run and divided into two steps (Step1 and Step2) due to different sample plug volumes in measure OD:

Initiation_Step1, SamplingandElution_Step1, Cleaning_Step1, PauseToSetTime_Step1, PauseUntilNextHour_Step1, Loop_Step1, Initation_Step2, SamplingandElution_Step2, Cleaning_Step2, PauseToSetTime_Step2, PauseUntilNextHour_Step2 and Loop_Step2.

At first, the sample plug for MeasureOD_Step1 was set to 80 µl and 40 µl in Step2. Afterwards the number of loops in Loop_Step2 and volumes in MueasureOD_Step2 was variated according to previously described. After the entire run the number of loops in Loop_Step2 was changed to 1 and started from Initiation_Step2 so that an extra measurement could be made.

Appendix D

Displayed in Figured D1 is an outtake of a previous fermentation. The x-axel only states a sampling point and not a time. The measurements are hourly. (Blue = online). The equation from the dilution curve was used to translate the volumes used into dilutions as they weren't of the volumes 40, 20 or 10 µl. Offline samples prior to the registration of the online samples are not displayed. The sampling tube hade a 0.25 mm diameter and pulled in sampled at a rate of 1.67 µl/s. Only the sequential online samples are displayed below, if air bubbles disturbed or there as a gap in the sampling, the measurements were excluded.

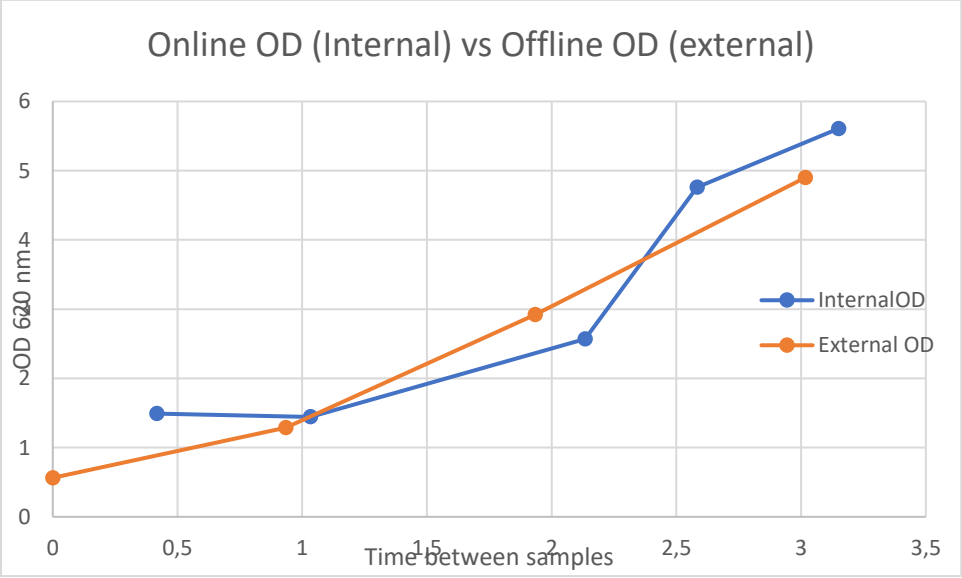

Figure D1. Online OD (blue) vs Offline Cell OD (orange). The x-axis does not represent the hours after induction, start for the time comparison is OD 0.564 for the offline samples.

Figure D1 is based on the fitted curve in Figure 6 and the measured OD at each volume presented in Table D2.

Table D2. OD at 620 nm, dilution and calculated OD from online fermentation samples.

Volume [µl]	Measured OD	Calculated Dilutions	Calculated OD
112.5	0.484	3.08	1.49
112.5	0.468	3.08	1.044
50	0.39	6.58	2.57
37.5	0.552	8.62	4.76
18.75	0.34	16.49	5.61

Appendix E

Table E1 displays the total volume that was dispensed from the second loop to the dilution chamber. The volume that consisted of binding buffer and the volume needed to push the BBM plug from the loop to the dilution chamber are also listed. Based on the first three rows, the final volume BBM to reach the dilution chamber was calculated.

Table E1. Calculations based on error influence on lysis.

Total Volume Dispensed [µl]	135
Volume Binding Buffer in loop [µl]	45
Volume Needed to Reach Dilution Chamber [µl]	12
Calculated Volume BBM in Dilution Chamber [µl]	75

Appendix F

A segment of an alternative sampling and elution scheme to the sampling and elution scheme described below. The sampling tube and BBM tube have since this scheme been replaced with 0.25 mm diametric tubes. Additionally, the equilibrated and calibration of the system is performed in this sub-schedule instead of the Initiation schedule. There are other differences, however the limitation is set to just the mixing of BBM and sample.

1. PrepareConfluentPointWithBugBuster:
   Uses VPSe to dispense 45 µl of BBM from Pump ID 3, Valve ID 4, through port 3 at a flow 0f 10 µl per second.
2. Two VPSe schemes are active simultaneously. One is pump ID 3 and valve ID 4 dispensing 135 µl of BBM at 5 µl/s through port 3 to the confluent point. The second one is the scheme dispensing 95 µl of (75µl sample and, the remaining volume, running buffer) to the confluent point at 5µl/s.
3. The system pauses until Tecan 3 and 4 have completed the task.

Appendix G

The eluted proteins form the fermentation after SDS-Page are displayed in Figure G1. No bands are seen for the eluted protein, only for pure protein G and the molecular weight ladders.

Figure G1. Online fermentation purified protein from fermentation.

Appendix H

The different OD measurements from the first to the last sampling point of the fermentation are listed in Figures H1 to H8, covering sampling points 1 – 9. The images display the internal UV-detection.

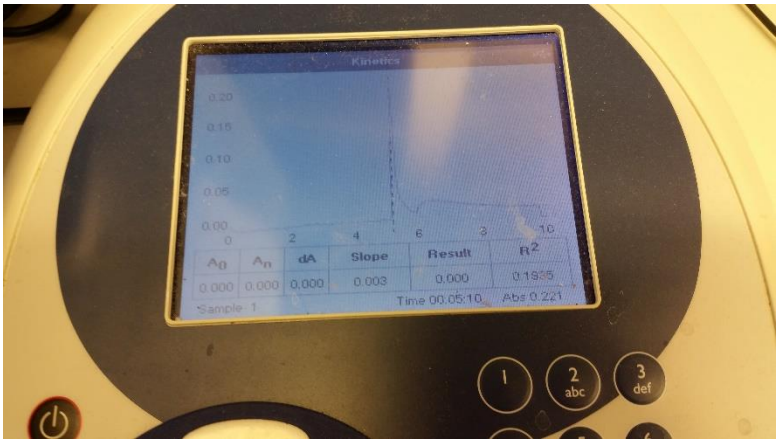

Figure H1. Sampling point 1.

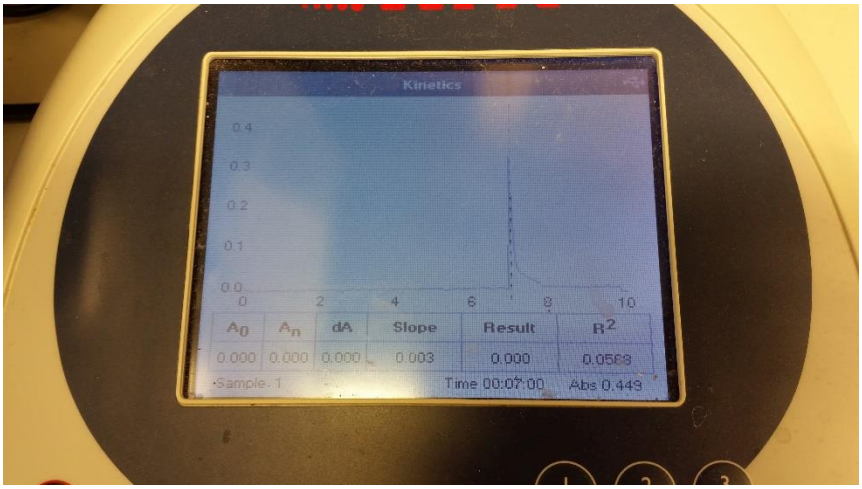

Figure H2. Sampling point 2.

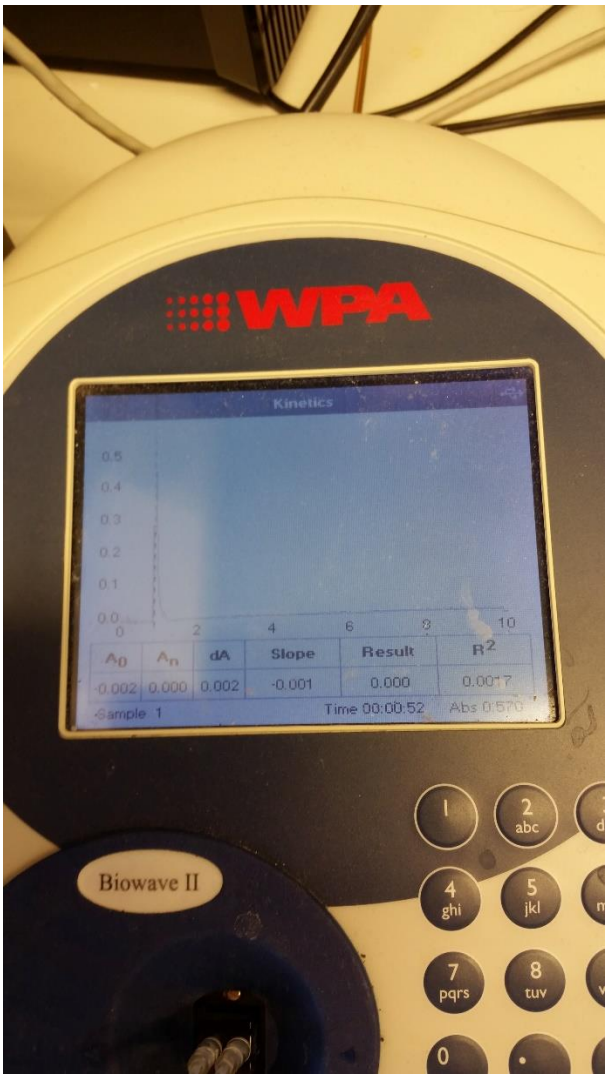

Figure H3. Sampling point 3.

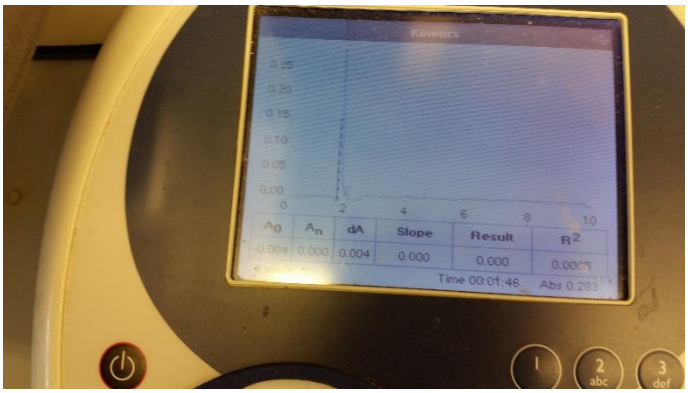

Figure H4. Sampling point 4.

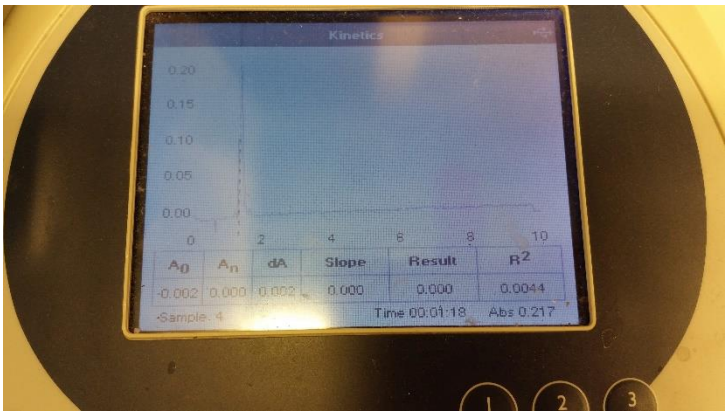

Figure H5. Sampling point 6.

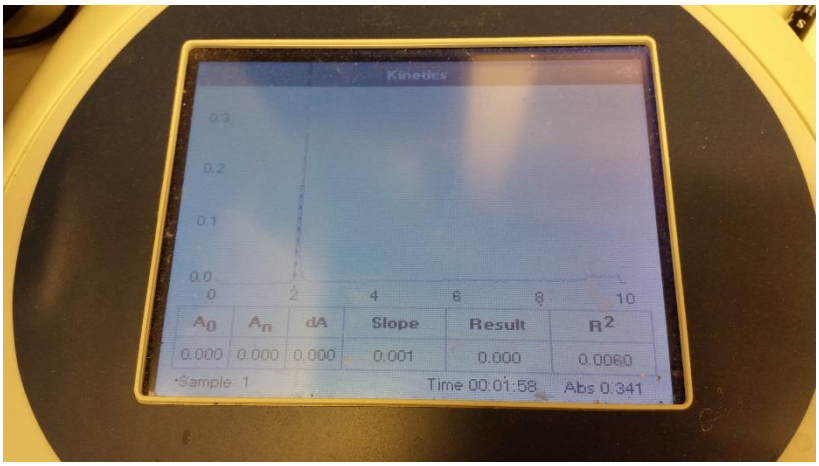

Figure H6. Sampling point 7.

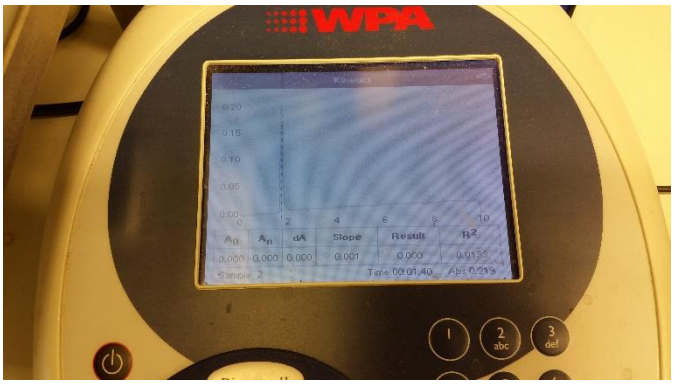

Figure H7. Sampling point 8.

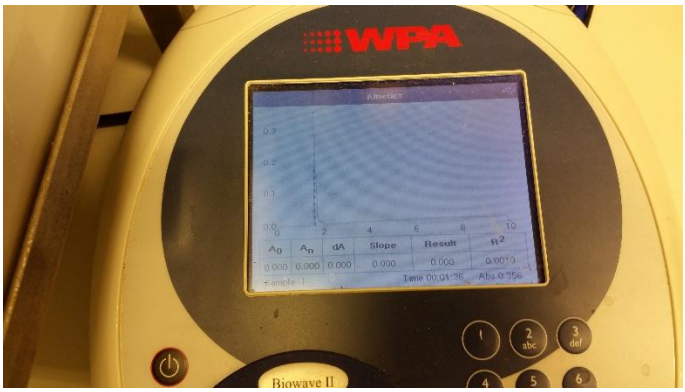

Figure H8. Sampling point 9.

Appendix I

Table I1 displays the distribution of the different samples and standard concentrations. P stands for pure protein G stock. The concentration of pure protein G stock ranges from approximately 0.625 to 10.0 µg/ml. S stands for sample and EB for eluted protein.

Table I1. Distribution of protein samples. *1 indicates pipetting error and should be discarded.

	1	2	3	4	5	6	7	8	9	10	11	12
A	S1 EB1	S2 EB1	S3 EB1	S4 EB1	S5 EB1	S6 EB1	S7 EB1	S8 EB1	S9 EB1	P 0.625 mg/ml	P 1.25 mg/ml	2.5 mg/ml
B												
C			*1									
D												
E												
F	5.0 mg/ml		*1									
G	10.0 mg/ml											
H									Blank			

The distribution of the dilutions of the samples are displayed in table H2. Either a times-two dilutions or a 3.3 dilutions was used.

Table I2. The dilutions of the samples are displayed. Orange is for a 2 times dilution and red for a 3.3 dilution of the samples.

	1	2	3	4	5	6	7	8	9	10	11	12
A	x2 dilution											
B	x2 dilution											
C	x 3.3 dilution											
D	x 3.3 dilution											
E	x 3.3 dilution											
F												
G												
H												

Tables I3 through I9 displayed the measured signals from the ELISA during time 0, 6, 15, 24, 33, 60, 120 minutes.

Table I3. Measured signals at time 0 minutes.

	1	**2**	**3**	**4**	**5**	**6**	**7**	**8**	**9**	**10**	**11**	**12**
A	0.076	0.074	0.077	0.087	0.078	0.072	0.077	0.081	0.079	0.083	0.082	0.079
B	0.076	0.07	0.074	0.077	0.076	0.075	0.075	0.079	0.082	0.081	0.098	0.08
C	0.077	0.074	0.073	0.078	0.076	0.071	0.075	0.071	0.081	0.082	0.084	0.085
D	0.076	0.076	0.077	0.081	0.079	0.075	0.076	0.079	0.078	0.079	0.083	0.084
E	0.081	0.08	0.078	0.078	0.036	0.034	0.04	0.037	0.033	0.083	0.084	0.088
F	0.079	0.081	0.081	0.084	0.082	0.038	0.041	0.045	0.042	0.041	0.039	0.039
G	0.082	0.079	0.08	0.081	0.081	0.037	0.037	0.04	0.036	0.034	0.038	0.037
H	0.042	0.042	0.037	0.043	0.038	0.041	0.036	0.077	0.076	0.077	0.077	0.075

Table I4. Measure signal after 6 minutes.

	1	**2**	**3**	**4**	**5**	**6**	**7**	**8**	**9**	**10**	**11**	**12**
A	0.08	0.077	0.077	0.092	0.079	0.073	0.079	0.086	0.079	0.089	0.086	0.088
B	0.079	0.072	0.076	0.077	0.078	0.077	0.076	0.079	0.084	0.084	0.086	0.087
C	0.08	0.075	0.073	0.079	0.076	0.072	0.078	0.072	0.082	0.085	0.091	0.096
D	0.082	0.079	0.079	0.084	0.079	0.076	0.078	0.081	0.077	0.082	0.086	0.094
E	0.083	0.08	0.081	0.079	0.036	0.034	0.039	0.036	0.033	0.086	0.087	0.099
F	0.089	0.082	0.092	0.101	0.09	0.036	0.039	0.045	0.043	0.04	0.034	0.037
G	0.101	0.088	0.092	0.086	0.087	0.033	0.037	0.04	0.031	0.03	0.031	0.036
H	0.041	0.041	0.043	0.041	0.036	0.039	0.035	0.077	0.076	0.079	0.078	0.077

Table I5. Measured signal after 15 minutes.

	1	**2**	**3**	**4**	**5**	**6**	**7**	**8**	**9**	**10**	**11**	**12**
A	0.081	0.077	0.079	0.094	0.081	0.074	0.079	0.091	0.079	0.096	0.091	0.101
B	0.082	0.073	0.077	0.08	0.079	0.077	0.077	0.08	0.084	0.086	0.088	0.103
C	0.081	0.076	0.074	0.08	0.077	0.073	0.081	0.072	0.082	0.087	0.098	0.114
D	0.082	0.08	0.08	0.086	0.08	0.077	0.078	0.082	0.077	0.084	0.085	0.105
E	0.086	0.082	0.084	0.08	0.036	0.034	0.039	0.037	0.034	0.088	0.092	0.108
F	0.11	0.113	0.106	0.115	0.102	0.034	0.036	0.045	0.042	0.039	0.032	0.037
G	0.131	0.139	0.133	0.12	0.131	0.031	0.035	0.039	0.029	0.029	0.03	0.036
H	0.041	0.04	0.042	0.04	0.036	0.037	0.034	0.077	0.077	0.079	0.079	0.077

Table I6. Measured signal after 24 minutes.

	1	**2**	**3**	**4**	**5**	**6**	**7**	**8**	**9**	**10**	**11**	**12**
A	0.082	0.077	0.081	0.095	0.082	0.075	0.081	0.093	0.08	0.1	0.094	0.106
B	0.083	0.074	0.079	0.08	0.08	0.077	0.078	0.08	0.083	0.087	0.089	0.105
C	0.082	0.078	0.076	0.08	0.077	0.073	0.082	0.073	0.082	0.088	0.099	0.126
D	0.083	0.082	0.081	0.088	0.081	0.077	0.079	0.082	0.078	0.088	0.089	0.111
E	0.086	0.084	0.085	0.08	0.035	0.033	0.039	0.036	0.034	0.091	0.094	0.11
F	0.131	0.133	0.121	0.137	0.118	0.034	0.036	0.044	0.042	0.039	0.032	0.036
G	0.186	0.188	0.167	0.141	0.167	0.031	0.037	0.04	0.029	0.029	0.029	0.036
H	0.041	0.04	0.041	0.04	0.036	0.037	0.034	0.078	0.077	0.078	0.079	0.078

Table I7. Measured signal after 33 minutes.

	1	**2**	**3**	**4**	**5**	**6**	**7**	**8**	**9**	**10**	**11**	**12**
A	0.083	0.078	0.083	0.096	0.084	0.076	0.081	0.094	0.08	0.103	0.095	0.108
B	0.085	0.078	0.08	0.081	0.081	0.079	0.078	0.08	0.083	0.088	0.09	0.109
C	0.084	0.08	0.077	0.081	0.078	0.074	0.083	0.073	0.082	0.089	0.1	0.13
D	0.085	0.084	0.082	0.088	0.081	0.078	0.08	0.083	0.078	0.088	0.092	0.115
E	0.087	0.085	0.087	0.081	0.035	0.033	0.039	0.037	0.034	0.092	0.095	0.118
F	0.149	0.15	0.134	0.154	0.135	0.034	0.036	0.044	0.041	0.039	0.032	0.037
G	0.213	0.213	0.191	0.162	0.203	0.032	0.037	0.039	0.029	0.029	0.029	0.036
H	0.042	0.04	0.04	0.04	0.036	0.037	0.034	0.079	0.078	0.079	0.081	0.078

Table I8. Measured signal after 60 minutes.

	1	**2**	**3**	**4**	**5**	**6**	**7**	**8**	**9**	**10**	**11**	**12**
A	0.09	0.084	0.089	0.099	0.088	0.08	0.081	0.098	0.083	0.11	0.098	0.115
B	0.093	0.081	0.084	0.084	0.083	0.082	0.08	0.082	0.083	0.089	0.095	0.115
C	0.091	0.086	0.08	0.083	0.079	0.075	0.085	0.075	0.083	0.091	0.103	0.138
D	0.092	0.088	0.086	0.092	0.083	0.079	0.081	0.084	0.08	0.09	0.097	0.122
E	0.095	0.09	0.091	0.083	0.035	0.033	0.039	0.037	0.034	0.095	0.099	0.12
F	0.184	0.173	0.159	0.176	0.154	0.036	0.04	0.044	0.04	0.039	0.034	0.037
G	0.258	0.258	0.238	0.189	0.246	0.034	0.038	0.04	0.03	0.031	0.031	0.036
H	0.046	0.04	0.04	0.042	0.037	0.039	0.036	0.082	0.081	0.081	0.084	0.081

Table I9. Measured signal after 120 minutes.

	1	2	3	4	5	6	7	8	9	10	11	12
A	0.111	0.097	0.103	0.106	0.098	0.087	0.085	0.107	0.088	0.118	0.101	0.119
B	0.109	0.092	0.092	0.088	0.088	0.085	0.083	0.085	0.085	0.091	0.1	0.119
C	0.108	0.095	0.088	0.089	0.083	0.079	0.089	0.077	0.085	0.093	0.104	0.143
D	0.109	0.099	0.093	0.097	0.086	0.082	0.083	0.086	0.082	0.091	0.1	0.127
E	0.111	0.101	0.098	0.088	0.034	0.033	0.039	0.037	0.034	0.097	0.101	0.121
F	0.208	0.186	0.173	0.185	0.163	0.036	0.039	0.044	0.04	0.039	0.033	0.037
G	0.275	0.269	0.25	0.197	0.26	0.034	0.039	0.04	0.03	0.032	0.032	0.036
H	0.05	0.041	0.041	0.043	0.038	0.039	0.036	0.09	0.086	0.085	0.089	0.089

The difference between sampling time zero and sampling time 120 minutes are displayed in table I10. In the figure, the yellow squares represent the standard curve, the orange squares the x2 diluted samples, the red squares the x3.3 diluted samples. Green squares represent the blank and blue squares display either empty or contaminated boxes.

Table I10. The difference between the measurement after 120 minutes subtracted by the signal measured after 0 minutes.

	1	2	3	4	5	6	7	8	9	10	11	12
A	0.035	0.023	0.026	0.019	0.02	0.015	0.008	0.026	0.009	0.035	0.019	0.04
B	0.033	0.022	0.018	0.011	0.012	0.01	0.008	0.006	0.003	0.01	0.002	0.039
C	0.031	0.021	0.015	0.011	0.007	0.008	0.014	0.006	0.004	0.011	0.02	0.058
D	0.033	0.023	0.016	0.016	0.007	0.007	0.007	0.007	0.004	0.012	0.017	0.043
E	0.03	0.021	0.02	0.01	-0.002	-0.001	-0.001	0	0.001	0.014	0.017	0.033
F	0.129	0.105	0.092	0.101	0.081	-0.002	-0.002	-0.001	-0.002	-0.002	-0.006	-0.002
G	0.193	0.19	0.17	0.116	0.179	-0.003	0.002	0	-0.006	-0.002	-0.006	-0.001
H	0.008	-0.001	0.004	0	0	-0.002	0	0.013	0.01	0.008	0.012	0.014

Appendix J

The estimated amount of protein lysed and eluted if the fermentation had been of a high-density nature based on discussed assumption of cell lysis after identified error. The calculations are based on the purified amount of protein G from a litre fermentation (Zhang, et al., 2015). The molecular weight for recombinant protein G is 21.6 g/mol (ThermoFisher Scientific, n.d.). The amount of protein G produced based on the listed approximations are displayed in Table J1.

Table J1. Calculations on amount of lysed protein G purified during fermentation as a result of the error. Based on assumption.

Protein G [g/L] from literature	Volume sample injected [µl]	Percentage lysed [%]	Amount of protein released [µg]	Conversion from g to moles (mol)
1	75	38.9	29.2	1.35e-6

Appendix K

The average measured OD from the internal online UV-detector in relation to the volume of *E.coli* injected into the internal UD-detector are displayed in Figure K1. In addition, the standard deviations are also represented in the figure below.

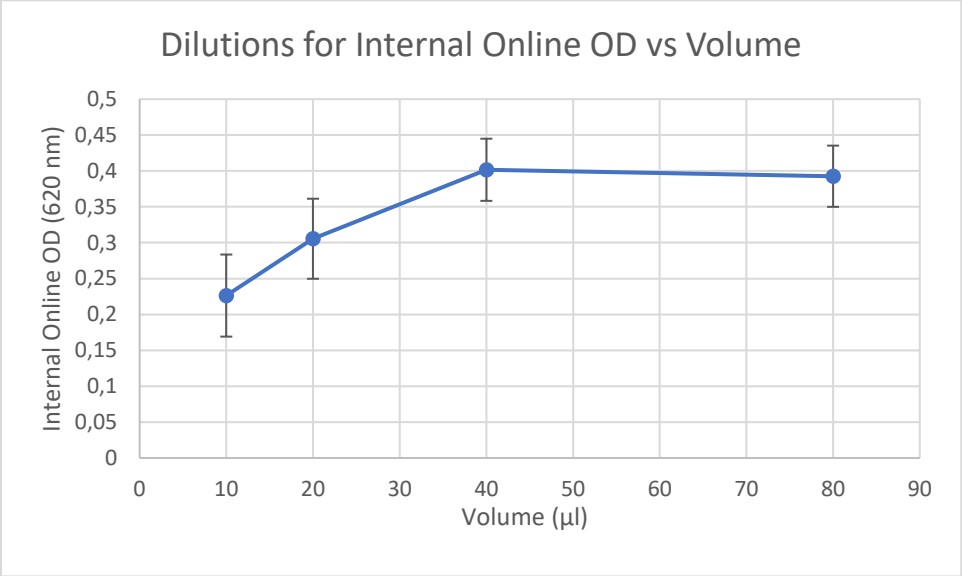

Figure K1. The measured OD at 620 nm from the different volumes used in the dilution study. The data-points are the average. Additionally, standard deviations are represented as error-bars.

Appendix L

OD and glucose measurements from the final fermentation are displayed in Appendix L.
In Table L1 the OD measurements at 620 nm are displayed. The measurements are recalculated after dilutions made. Potassium phosphate buffer (10 mM) was used to dilute the cells.

Table L1. Offline OD measurements at 620 nm.

Time after Inoculation (h)	OD Measured	Dilution	OD Recalculated
0	0,482	1	0,482
1,216667	0,686	2	1,372
2,15	0,222	10	2,22
2,616667	0,333	10	3,33
4,233333	0,203	20	4,06
5,183333	0,264	20	5,28
6,25	0,3	20	6
7,266667	0,344	20	6,88
8,35	0,353	20	7,06

The online external OD measurements are assumed to have occurred within minutes of the time after inoculation and follow the same time points as the offline measurements. Table L2 displays the collected data. At the fifth sampling point no measurement was made.

Table L2. Measured online external OD at 620 nm. Recalculated OD depending on injected sample volume is also displayed.

Time after Inoculation (h)	Measured OD	Volume Sample (µl)	Recalculated OD
0	0,221	80	1,128642
1,216667	0,449	80	2,293034
2,15	0,57	40	3,794323
2,616667	0,283	20	3,714664
4,233333	-	-	-
5,183333	0,217	10	7,68929
6,25	0,341	10	12,08317
7,266667	0,219	10	7,760159
8,35	0,356	10	12,61469

The glucose measurements are displayed in Table L3. Dilutions were made using MQ-water.

Table L3. Glucose measurements from the final fermentation.

Sampling Point	Glucose Concentration (mmol/L)	Dilution	Recalculated Glucose Concentration (mmol/L)
1	3.3	10	33
2	2.5	10	25
3	2.1	10	21
4	11.6	1	11.6
5	4.4	1	4,4
6	4.1	1	4.1
7	5.1	1	5.1
8	7.4	1	7.4
9	7.3	1	7.3